CHEMISTRY
A EUROPEAN JOURNAL

DOI: 10.1002/chem.201000777

Bistable or Oscillating State Depending on Station and Temperature in Three-Station Glycorotaxane Molecular Machines

Eric Busseron, Camille Romuald, and Frédéric Coutrot*[a]

Abstract: High-yield, straightforward synthesis of two- and three-station [2]rotaxane molecular machines based on an anilinium, a triazolium, and a mono- or disubstituted pyridinium amide station is reported. In the case of the pH-sensitive two-station molecular machines, large-amplitude movement of the macrocycle occurred. However, the presence of an intermediate third station led, after deprotonation of the anilinium station, and depending on the substitution of the pyridinium amide, either to exclusive localization of the macrocycle around the triazolium station or to oscillatory shuttling of the macrocycle between the triazolium and monosubstituted pyridinium amide station. Variable-temperature ^{1}H NMR investigation of the oscillating system was performed in CD_2Cl_2. The exchange between the two stations proved to be fast on the NMR timescale for all considered temperatures (298–193 K). Interestingly, decreasing the temperature displaced the equilibrium between the two translational isomers until a unique location of the macrocycle around the monosubstituted pyridinium amide station was reached. Thermodynamic constants K were evaluated at each temperature: the thermodynamic parameters ΔH and ΔS were extracted from a Van't Hoff plot, and provided the Gibbs energy ΔG. Arrhenius and Eyring plots afforded kinetic parameters, namely, energies of activation E_a, enthalpies of activation $\Delta H^{\neq}$, and entropies of activation $\Delta S^{\neq}$. The ΔG values deduced from kinetic parameters match very well with the ΔG values determined from thermodynamic parameters. In addition, whereas signal coalescence of pyridinium hydrogen atoms located next to the amide bond was observed at 205 K in the oscillating rotaxane and at 203 K in the two-station rotaxane with a unique location of the macrocycle around the pyridinium amide, no separation of ^{1}H NMR signals of the considered hydrogen atoms was seen in the corresponding nonencapsulated thread. It is suggested that the macrocycle acts as a molecular brake for the rotation of the pyridinium–amide bond when it interacts by hydrogen bonding with both the amide NH and the pyridinium hydrogen atoms at the same time.

Keywords: molecular devices · rotaxanes · supramolecular chemistry

Introduction

Rotaxanes and catenanes have been the subject of extensive research during the past decade, especially because such interlocked compounds can be used as mechanical or electronic molecular devices in the field of nanotechnology.[1] Many rotaxanes incorporating dibenzo[24]crown-8 (DB24C8) as the macrocycle and cationic moieties as templates have already been published. Since Bush et al. reported the ability of DB24C8 to interact strongly with ammonium,[2] other templates such as benzylic ammonium,[3] *N*-benzylic anilinium,[4] *N,N'*-dialkyl-4,4'-bipyridinium,[5] and 1,2-bis(pyridinium)ethane cations[6] have been described. As part of our ongoing studies concerning the synthesis of glycorotaxane[7] molecular shuttles, we reported three new molecular stations for DB24C8.[8] Triazolium and mono- or disubstituted pyridinium amide moieties separately appeared to be poorer molecular stations for DB24C8 than anilinium. However, no rotaxane molecular machine incorporating the three different stations was reported so far. Hence, no knowledge about the relative binding affinity of each station for DB24C8 was available. Herein we report on the synthesis of molecular machines containing an anilinium, a *N*-methyltriazolium, and either a mono- or a disubstituted pyridinium amide sta-

[a] Dr. E. Busseron, C. Romuald, Dr. F. Coutrot
Institut des Biomolécules Max Mousseron (IBMM)
UMR 5247 CNRS-Universités Montpellier 2 et 1
Bâtiment de Recherche Max Mousseron
Ecole Nationale Supérieure de Chimie de Montpellier
8, rue de l'Ecole Normale, 34296 Montpellier Cedex 5 (France)
Fax: (+33) 467-14-43-44
E-mail: frederic.coutrot@univ-montp2.fr

Supporting information for this article is available on the WWW under http://dx.doi.org/10.1002/chem.201000777.

View this journal online at wileyonlinelibrary.com

© 2010 Wiley-VCH Verlag GmbH & Co. KGaA, Weinheim

tion. Unsurprisingly, in the protonated anilinium state, DB24C8 resides around the best anilinium station. The shuttling behaviors of the two different systems upon deprotonation were then studied by ^{1}H NMR spectroscopy and found to directly depend on the relative binding affinity of these stations for DB24C8. In the presence of the triazolium and the disubstituted pyridinium amide stations, deprotonation of the anilinium station causes DB24C8 to shuttle toward the sole triazolium station. However, with the mono-substituted pyridinium amide, very close binding affinity of the DB24C8 for the two stations was observed; thus, after deprotonation, continuous oscillating movement of the macrocycle between the two sites of interaction occurs. A variable-temperature ^{1}H NMR study on the oscillating molecular shuttle demonstrated that decreasing the temperature displaces the equilibrium between the two translational isomers, in fast exchange on the NMR timescale, towards the isomer with DB24C8 around the mono-substituted pyridinium amide. Thermodynamic and kinetic parameters were extracted from the ^{1}H NMR experiments, and allowed the determination of energies and enthalpies of activation E_a and $\Delta H^{\neq}$, entropies $\Delta S^{\neq}$, free enthalpies of activation $\Delta G^{\neq}$, and free enthalpies of exchange ΔG. Very small ΔG of exchange was found at room temperature between the two translational isomers, which corroborates the very similar binding affinity of DB24C8 for both the triazolium and the mono-substituted pyridinium amide, although with a very faint preference for location of DB24C8 around the mono-substituted pyridinium amide station. It was also observed that DB24C8 acts as a molecular brake[9] by slowing down rotational isomerization of the pyridinium amide when it is located around the pyridinium amide site.

Results and Discussion

Synthesis and molecular machinery of two-station [2]rotaxanes 3a,b: Rotaxanes **3** were synthesized from the previously prepared mono- or disubstituted mannosyl pyridinium amide azide **1** and ammonium compound **2** by copper(I)-catalyzed Huisgen[10] alkyne–azide 1,3-dipolar cycloaddition, also known as CuAAC click chemistry[11] (Scheme 1).

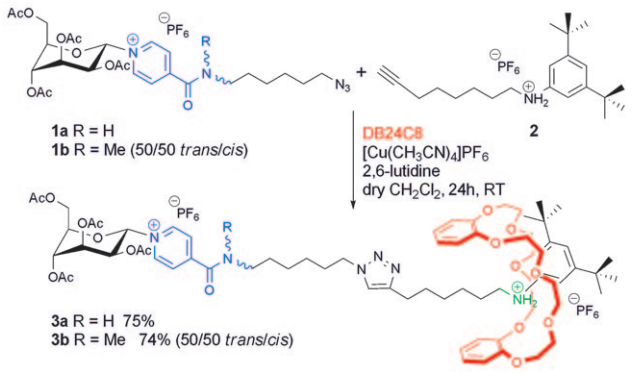

Scheme 1. Synthesis of rotaxanes **3a** and **3b**.

The reaction was carried out in dichloromethane at ambient temperature over 24 h with DB24C8 (2 equiv), azido compound **1** (1 equiv), alkyne **2** (1 equiv), $Cu(MeCN)_4PF_6$ (1 equiv), and 2,6-lutidine (0.1 equiv). In the case of the rotaxane **3b**, a 1:1 mixture of two stereoisomers was observed due to *cis*/*trans* isomerism of the disubstituted amide. Interestingly, no formation of [3]rotaxane occurred under these experimental conditions, that is, the binding affinity of the two pyridinium amide moieties for DB24C8 is very poor.

We recently reported an ^{1}H NMR study of the molecular machinery of two-station rotaxanes **3a** and **3b** with variations in pH.[8c] The anilinium moiety was found to be the best molecular station for DB24C8. Therefore, the macrocycle resides exclusively around the anilinium moiety at low pH. Deprotonation of **3** was carried out by adding an excess (5 equiv) of diisopropylethylamine (DIEA) at room temperature (Scheme 2), and brings about a large-amplitude displacement of DB24C8 from one extremity of the molecule to the other. The macrocycle sits around the mono- or the disubstituted pyridinium amide station, respectively, in **4a** or **4b** (Scheme 2). The mannosyl end proved to be sufficiently cumbersome to prevent any disassembly of the interlocked architecture. The location of the macrocycle around the pyridinium moiety differs slightly depending on the substitution of the amide. Indeed, in the mono-substituted series **4a**, DB24C8 interacts by hydrogen bonding with H^8 and H^{11}. However, in the disubstituted series **4b**, DB24C8 does not interact at all with H^8: instead, it prefers to interact with hydrogen atoms H^7, which are actually closer to the cationic charge. In this latter case, we observed flipping of the chair-like mannopyranosyl ring from the $^1C_4$ to the $^4C_1$ conformation, as a result of turning off of the reverse anomeric effect.[12] Although this study allows the relative binding affinity of the anilinium and the pyridinium amide stations for DB24C8 to be ranked, no information about the relative affinity of DB24C8 for the triazolium and either mono- or disubstituted pyridinium amide was known. We thus envisaged introduction of the triazolium moiety between the two previously studied molecular stations.

Synthesis of three-station [2]rotaxanes 5a,b: Regioselective N-alkylation of the 1,4-disubstituted-1,2,3-triazole moiety with iodomethane provided, after counteranion exchange, triazolium rotaxanes **5a** and **5b**[13] in 93 and 91 % yield, respectively (Scheme 2).

Each [2]rotaxane molecular machine **5a** and **5b** now contains three different sites of interaction for DB24C8: anilinium, triazolium, and mono- or disubstituted pyridinium amide. Possible shuttling of the macrocycle upon deprotonation of the anilinium station was then explored, with the aim of evaluating the relative affinity of DB24C8 for the pyridinium amide and triazolium moieties (Scheme 2). It was of particular interest to study these relative affinities in the interlocked rotaxane structures, since intermolecular interactions between pyridinium amide or triazolium templates did not prove to be strong enough to allow the detection of semirotaxanes. Upon deprotonation of starting rotaxanes **5a**

 © 2010 Wiley-VCH Verlag GmbH & Co. KGaA, Weinheim

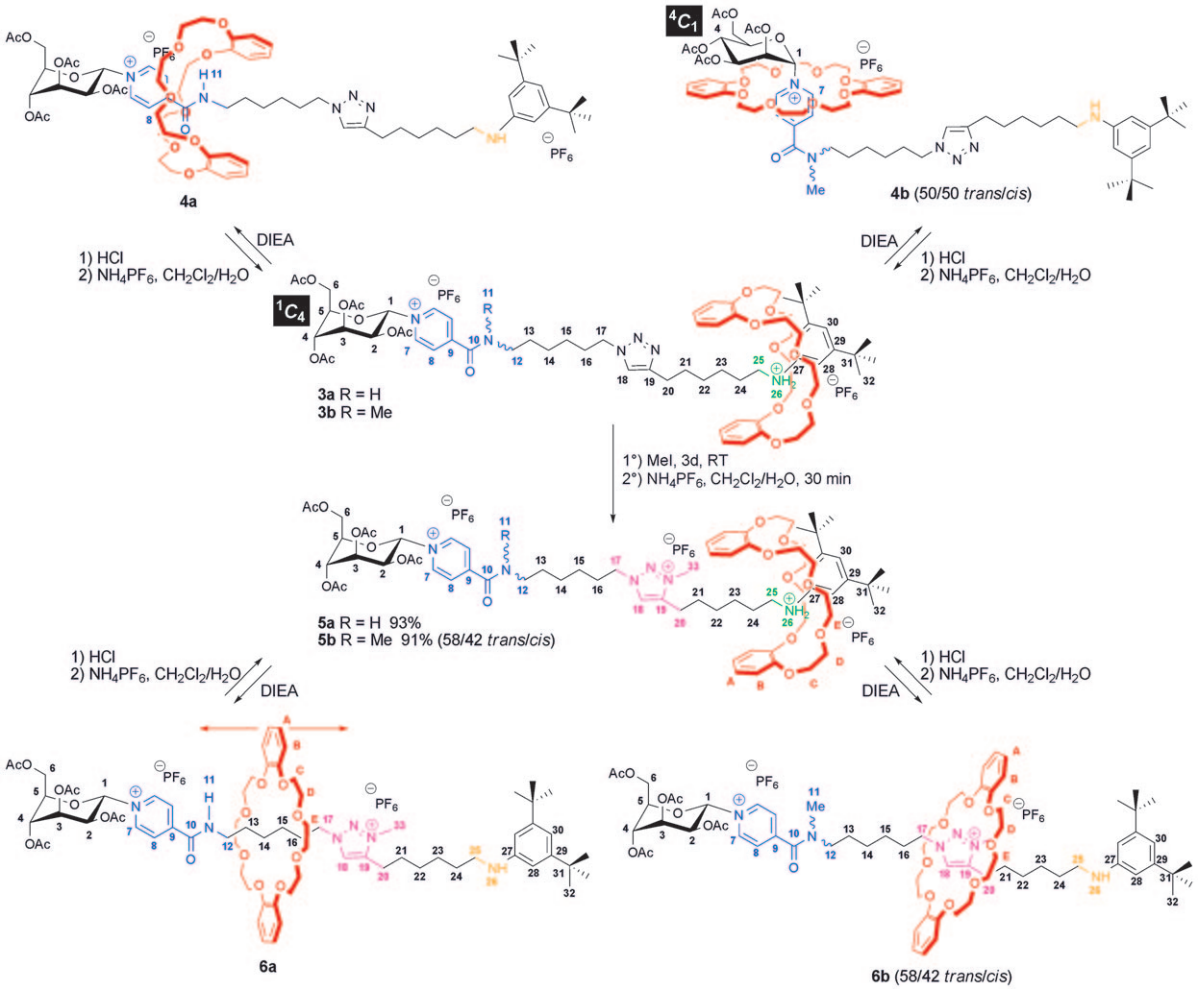

Scheme 2. Synthesis of **5a** and **5b**, and molecular machinery by deprotonation/protonation of rotaxanes **3a**, **3b**, **5a**, and **5b**.

and **5b** (Scheme 2, Figure 1b and c; and Figure 2b and c), the macrocycle moved from its anilinium initial position, but behaved very differently depending on the substitution of the pyridinium amide station.

Molecular machinery on rotaxanes 5b/6b by acid–base reaction: In the disubstituted pyridinium amide series, the molecular machine behaves as a pH-sensitive bistable [2]rotaxane in which the macrocycle shuttles between the anilinium and triazolium stations. Superimposition of the ^{1}H NMR spectra for rotaxanes **5b/6b** with those of their corresponding nonencapsulated threads **5bu/6bu**[15] illustrates the molecular machinery (Figure 1).

The macrocycle initially resides around the best, anilinium station in **5b**, as is confirmed by direct comparison of ^{1}H NMR spectra of rotaxane **5b** and thread **5bu** (Figure 1a and b). The hydrogen atoms H^{25}, located next to the anilinium station, are shifted downfield in the rotaxane ($\Delta\delta = +0.99$ ppm), whereas H^{20}, H^{21-23}, and to a lesser extent H^{18} experience the shielding effect of the aromatic ring of DB24C8. No other variations in chemical shifts are noticed, which is consistent with the exclusive localization of DB24C8 around the anilinium station. After deprotonation, the new position of the macrocycle can be deduced by direct comparison between the ^{1}H NMR spectra of rotaxanes **5b** and **6b** (Figure 1b and c). The tremendous upfield shifts for H^{25} ($\Delta\delta = -1.06$ ppm), H^{28} ($\Delta\delta = -0.88$ ppm), and H^{30} ($\Delta\delta = -0.69$ ppm) in rotaxane **6b** results from deprotonation of the anilinium moiety and shuttling of the macrocycle. At the same time, the H^{18} is shifted downfield in **6b** ($\Delta\delta = +0.73$ ppm). The same trend is observed for H^{17} ($\Delta\delta = +0.46$ and $+0.52$ ppm), and to a lesser extent for H^{20} ($\Delta\delta = +0.20$ ppm). Interestingly, no other significant chemical variations of H signals are observed. These two observations unambiguously show that rotaxane **6b** behaves as a pH-sensitive bistable molecular machine. The macrocycle sits on the triazolium station after deprotonation, due to its better binding affinity for DB24C8 than the disubstituted pyridinium amide. The hydrogen atoms of the aliphatic chains located on both sides of the triazolium unit are more or less shifted upfield due to their location in the shielding cavity of the aromatic rings of DB24C8. The exclusive local-

 © 2010 Wiley-VCH Verlag GmbH & Co. KGaA, Weinheim

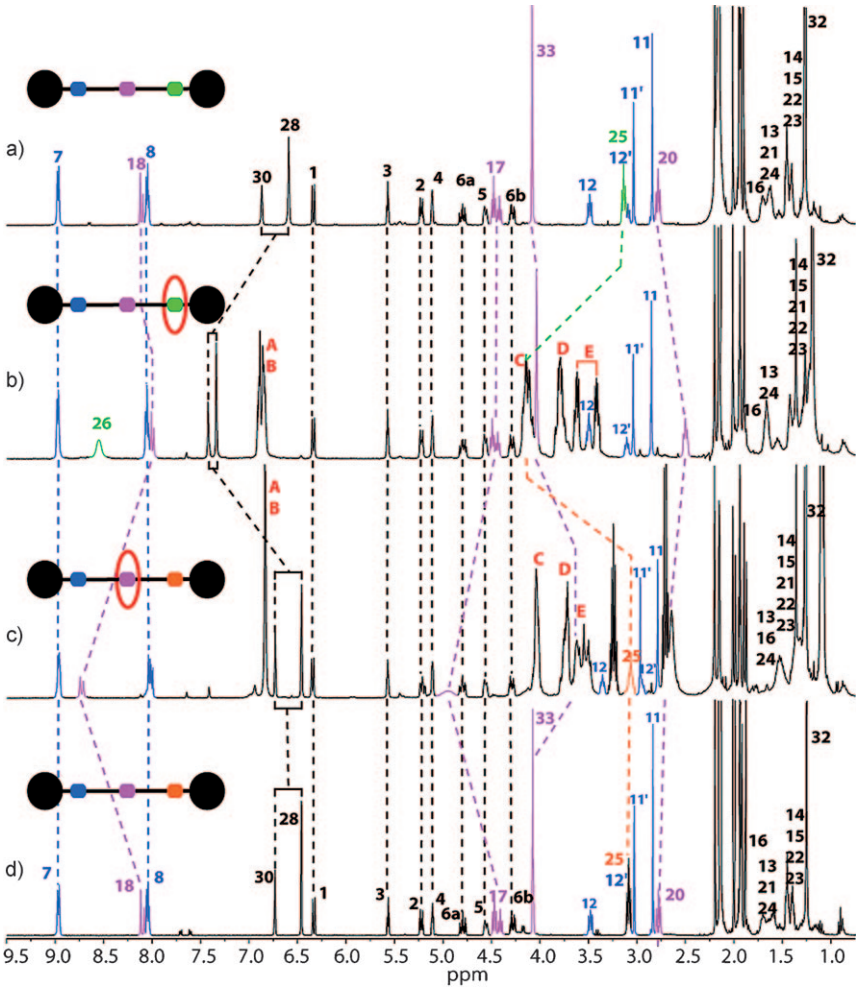

Figure 1. ^{1}H NMR spectra (400 MHz, CD_3CN, 298 K) of a) uncomplexed thread **5bu**, b) rotaxane **5b**, c) rotaxane **6b**, and d) thread **6bu**. The coloring, lettering, and numbering correspond to the proton assignments indicated in Scheme 2.

ization of the macrocycle around the triazolium station is corroborated by the comparison of the ^{1}H NMR spectra of deprotonated rotaxane **6b** with that of uncomplexed deprotonated thread **6bu** (Figure 1c-d). In rotaxane **6b**, H^{18} undergoes a downfield shift ($\Delta\delta = +0.61$ ppm), whereas no chemical shift variations are observed for pyridinium hydrogen atoms H^7 and H^8. Most of the other hydrogen atoms of the aliphatic chains are shielded in the rotaxane due to their location in the shielding cavity of the macrocycle.

This first study gave us information about the higher affinity of DB24C8 for the triazolium than for the disubstituted pyridinium amide station. We then extended our investigation to the case of a monosubstituted pyridinium amide.

Molecular machinery on three-station rotaxanes 5a/6a by acid–base reaction: In the monosubstituted pyridinium amide series, although the macrocycle resides again on the best anilinium station in protonated rotaxane **5a**, the macrocycle shuttles very differently after deprotonation. The shuttling in rotaxane **6a** behaves at room temperature as in a degenerate[14] molecular machine, whereby the macrocycle continuously oscillates between the triazolium and monosubstituted pyridinium amide stations (Figure 2).

This result suggests similar affinity of the two stations for DB24C8, in contrast to rotaxane **6b** containing a disubstituted pyridinium amide, wherein the macrocycle shuttles around the sole triazolium station (Figure 1). The ^{1}H NMR spectroscopic evidence for protonated and oscillating deprotonated states of the molecular machines **5a/6a** is reported in Figure 2. Similar to rotaxane **5b**, direct comparison of the ^{1}H NMR spectra of rotaxane **5a** and uncomplexed dumbbell-shaped thread **5au**[15] demonstrates the presence and the initial location of the DB24C8 around the anilinium station in **5a** (Figure 2a and b). Apart from the evident appearance of the signals corresponding to the hydrogen atoms of the macrocycle, hydrogen atoms H^{25} are shifted downfield in the rotaxane ($\Delta\delta = +1.01$ ppm) because of their hydrogen-bonding interactions with the oxygen atoms of DB24C8. Hydrogen atoms H^{20} and to a lesser extent H^{18} are shifted upfield ($\Delta\delta = -0.28$ and -0.11 ppm, respectively), because they probably experience the shielding effect of the aromatic ring of DB24C8. The same trend is observed for H^{21}–H^{23} belonging to the aliphatic chain ($\Delta\delta = -0.32$ and -0.26 ppm, respectively). Furthermore, no significant variations of the chemical shifts of the other hydrogen atoms are noticed, and especially those of the pyridinium amide moiety (H^7, H^8, and H^{11}) indicating the exclusive localization of DB24C8 around the anilinium station. Direct comparison of the ^{1}H NMR spectra of rotaxanes **5a** and **6a** reveals the new localizations of the macrocycle, which binds to both the triazolium and the pyridinium amide stations (Figure 2b and c). Hydrogen atoms H^{25} are now shifted upfield ($\Delta\delta = -1.06$ ppm) as a result of both deprotonation of the anilinium moiety and shuttling of the macrocycle. This is corroborated by the chemical-shift variations of the pyridinium amide and triazolium stations. Hydrogen atoms H^{18} and to a lesser extent H^{17} are shifted downfield ($\Delta\delta = +0.34$ and $+0.11$ ppm, respectively) in deprotonated rotaxane **6a**, and this is indicative of their involvement in hydrogen-bonding

 © 2010 Wiley-VCH Verlag GmbH & Co. KGaA, Weinheim

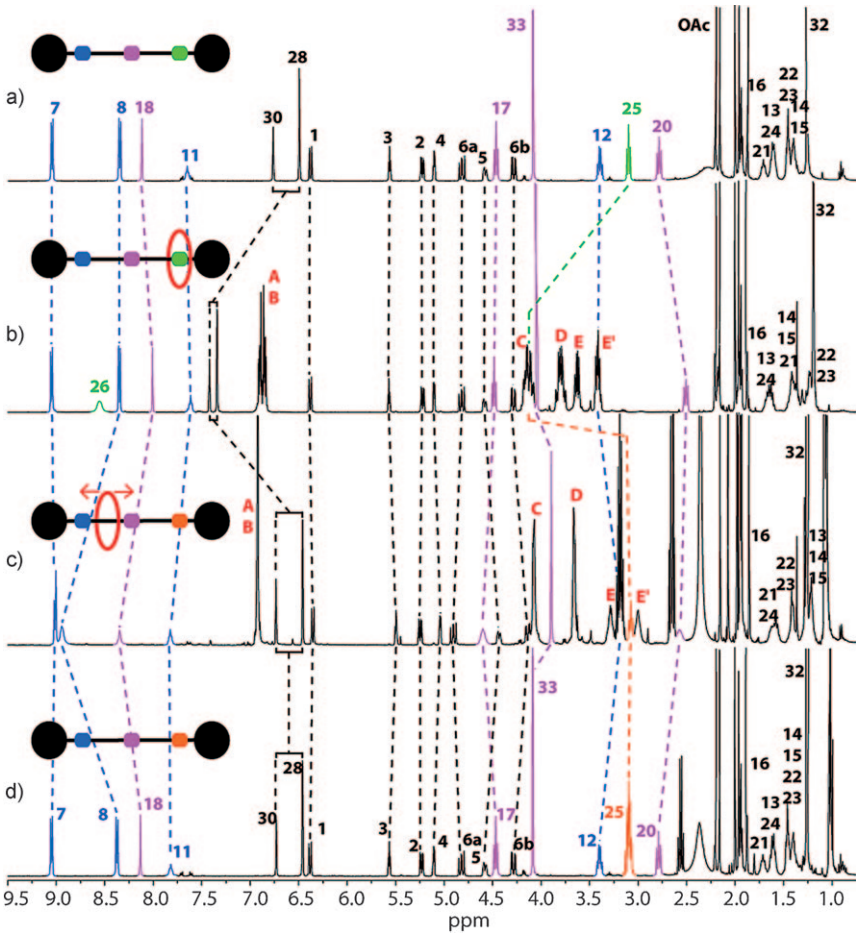

Figure 2. ^{1}H NMR spectra (400 MHz, CD_3CN, 298 K) of a) uncomplexed thread **5au**, b) rotaxane **5a**, c) rotaxane **6a**, and d) uncomplexed thread **6au**. The coloring, lettering, and numbering correspond to the proton assignments indicated in Scheme 2.

interactions with DB24C8. Meanwhile, hydrogen atoms H^8 and H^{11} of the pyridinium station are also shifted downfield ($\Delta\delta = +0.58$ and $+0.21$ ppm, respectively). Finally, the comparison of the ^{1}H NMR spectra of deprotonated rotaxane **6a** and uncomplexed dumbbell-shaped thread **6au** corroborates the two sites of interaction of DB24C8 observed in glycorotaxane molecular machine **6a** (Figure 2c and d). Even though the macrocycle binds to both stations, it is noteworthy that only one set of resonances was observed for **6a**. Moreover, and interestingly, the ^{1}H NMR signals of the hydrogen atoms which are engaged in hydrogen bonding with the macrocycle are broadened in **6a**. These two last observations suggest fast exchange between the two localizations of DB24C8 on the NMR timescale (Scheme 3).

Thus a deprotonated conformational state can be assumed in which the macrocycle oscillates quickly between the two stations on the NMR timescale. In this case, the observed ^{1}H NMR chemical shifts consist of the mole fraction weighted average of the chemical shifts in the two translational isomers of **6a**.[16] The observed ^{1}H NMR chemical shifts of H^8 and H^{18} of the two molecular stations that interact with the macrocycle in the oscillating rotaxane **6a** (Figure 3) are reported in Table 1.

The ^{1}H NMR chemical shifts δ_1 and δ_2 of H^8 and H^{18} in translational isomers $\mathbf{6a_1}$ and $\mathbf{6a_2}$ were estimated from the synthesized compounds shown in Figure 3 and allowed evaluation of the populations of translational co-conformers 1 and 2 of rotaxane **6a** (Table 1). On the one hand, chemical shifts of free hydrogen atoms H^8 and H^{18} were extracted from the ^{1}H NMR spectrum of the uncomplexed thread **5au**. On the other hand, chemical shifts of entirely H-bound hydrogen atoms H^8 and H^{18} were respectively extracted from rotaxane **4a**, in which the macrocycle exclusively interacts with the pyridinium amide station, and from the rotaxane **6b**, in which the macrocycle resides exclusively around the triazolium station. With this approximation, we consider, firstly, that there is no influence of the triazole and triazolium moieties on the chemical shift of H^8 of the pyridinium station, all other things being equal. Secondly, we assume that the same neutral effect should hold with regard to the effect of

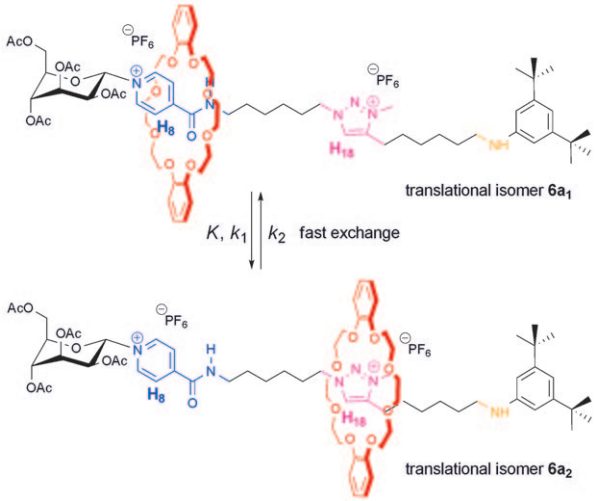

Scheme 3. Fast exchange between the two translational isomers $\mathbf{6a_1}$ and $\mathbf{6a_2}$ of rotaxane **6a**.

substitution of the amide on the chemical shift of H^{18} of the triazolium station. This assumption about the noninfluence of the substitution of the triazole on the chemical shift of H^8 (pyridinium station) and, in the same manner, of the substi-

 © 2010 Wiley-VCH Verlag GmbH & Co. KGaA, Weinheim

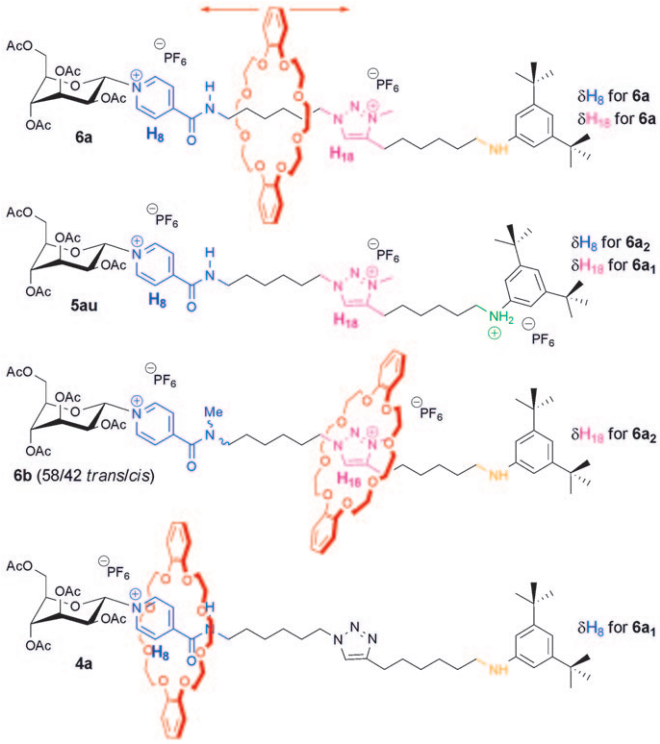

Figure 3. Considered compounds and hydrogen atoms for determination of the populations of translational isomers **6a$_1$** and **6a$_2$** in fast exchange on the NMR timescale.

Table 1. ^{1}H NMR (CD_3CN and CD_2Cl_2, 400 MHz) chemical shifts at variable temperature of selected hydrogen atoms of the triazolium and pyridinium stations, and deduced relative populations of translational isomers **6a$_1$**/**6a$_2$**.

Solvent	T [K]	δ_{H8} [ppm]			p [%]	δ_{H18} [ppm]			p [%]
		6a$_1$[a]	**6a$_2$**[b]	**6a**	**6a$_1$**/**6a$_2$**	**6a$_1$**[b]	**6a$_2$**[c]	**6a**	**6a$_1$**/**6a$_2$**
CD_3CN	298	9.31	8.36	8.93	60/40	8.12	8.73	8.34	64/36
CD_2Cl_2	298	9.36	8.45	8.98	58/42	8.15	8.81	8.40	62/38
	273	9.35	8.44	9.05	67/33	8.13	8.75	8.32	69/31
	263	9.34	8.43	9.08	71/29	8.11	8.74	8.29	71/29
	253	9.33	8.43	9.11	76/24	8.11	8.72	8.26	75/25
	243	9.36	8.42	9.16	79/21	8.09	8.70	8.23	77/23
	233	9.30	8.41	9.24	93/07	8.08	8.68	8.17	82/18
	223	9.29	8.41	9.29	100/00	8.06	8.66	8.10	93/07
	208	9.29	8.40	9.29	100/00	8.04	8.64	8.08	93/07
	205	9.28	8.39	–[d]	–	8.03	8.64	8.07	93/07
	193	9.27[e]	8.39	9.26[e]	99/01	8.01	8.62	8.06	92/08

[a] Measured on rotaxane **4a**, in which DB24C8 interacts exclusively with the monosubstituted pyridinium amide.[8c] [b] Measured on thread **5au**. [c] Measured on rotaxane **6b**, in which DB24C8 interacts exclusively with the triazolium station. [d] ^{1}H NMR signals of the two hydrogen atoms H^8 coalesce. [e] Average chemical shift from the two distinct signals in slow exchange on the NMR timescale.

tution of the pyridinium amide on the chemical shift of H^{18} (triazolium station) was perfectly verified with uncomplexed threads **4au**, **5au**, and **6bu** ($\Delta\delta H^8 = 0$ ppm between **4au** and **5au**; $\Delta\delta H^{18} < 0.01$ ppm between **4au** and **6bu**).

In CD_3CN at room temperature, an average ratio of translational isomers **6a$_1$**:**6a$_2$** in fast exchange of 62:38[17] was calculated and indicated continuous oscillation of DB24C8 between the monosubstituted pyridinium amide and triazolium stations with a faint preferential affinity of DB24C8 for the monosubstituted pyridinium amide station rather than for the triazolium station. Variation of the solvent polarity from CD_3CN to CD_2Cl_2 at room temperature did not modify significantly the population ratio **6a$_1$**:**6a$_2$**.

A variable-temperature ^{1}H NMR study was then conducted in CD_2Cl_2 by decreasing the temperature from 298 to 193 K: the chemical shifts of H^8 and H^{18} of the considered compounds **6a**, **5au**, **4a**, and **6b** clearly indicate a shift of the **6a$_1$**:**6a$_2$** equilibrium toward **6a$_1$**. Basically, upon decreasing the temperature, few variations are noticed for the evaluated chemical shifts of hydrogen atoms belonging to translational isomers **6a$_1$** and **6a$_2$**, whereas H^8 and H^{18} of the oscillating rotaxane **6a** are notably shifted downfield and upfield, respectively, until they reach a respective maximum and minimum at about 223 K (Table 1, Figure 4). These maximum and minimum clearly correspond to the chemical shifts of H-bound H^8 of rotaxane **4a** (i.e., H-bound H^8 of **6a$_1$**) and to free H^{18} of thread **5au** (i.e., free H^{18} of **6a$_1$**). Hence, the mean ratio **6a$_1$**:**6a$_2$** of 60:40 in CD_2Cl_2 at 298 K becomes 97:03 at 223 K.

Thermodynamic parameters of the fast exchange on the NMR timescale between translational isomers **6a$_1$** and **6a$_2$** were determined from the thermodynamic constant K, which was calculated at various temperatures from the ratios **6a$_1$**:**6a$_2$**. The Van't Hoff plot[18] ($\ln K$ versus $1/T$) was linear over the examined temperature range (233–298 K) with a linear regression coefficient of $R_2 = 0.997$,[19] and provided the translational isomeric exchange enthalpy from **6a$_1$** to **6a$_2$** of $\Delta H = 9.8$ kJ mol^{-1} and an entropy of $\Delta S = 29.6$ J K^{-1} mol^{-1} (Figure 5).

The positive value of ΔH shows that the translational movement of DB24C8 from the triazolium to the pyridinium station is enthalpy-driven. In addition, the positive variation of entropy for the exchange from **6a$_1$** to **6a$_2$** indicates the formation of a tighter complex pyridinium amide/DB24C8 **6a$_1$** with a better-defined geometry (i.e., a higher ordered structure with more restriction of motion). A free Gibbs energy ΔG (298 K) of 1.0 kJ mol^{-1} was found, which illustrates the very similar binding affinity of DB24C8 for the two stations, with a very faint preference for the pyridinium amide station.

The rate constants k_1 for movement of DB24C8 from the pyridinium amide to the triazolium station and k_2 for the opposite motion were determined from the broadening of the ^{1}H NMR signals of H^8 and H^{18}.[20] We used the equations $\Delta\nu = (4\pi p_1 p_2 \delta\nu^2)/(k_1 + k_2)$ and $p_1 k_1 = p_2 k_2$, where $\Delta\nu$ is the line broadening of the single resonance observed at the weighted average frequency for either H^8 or H^{18} in fast ex-

 © 2010 Wiley-VCH Verlag GmbH & Co. KGaA, Weinheim

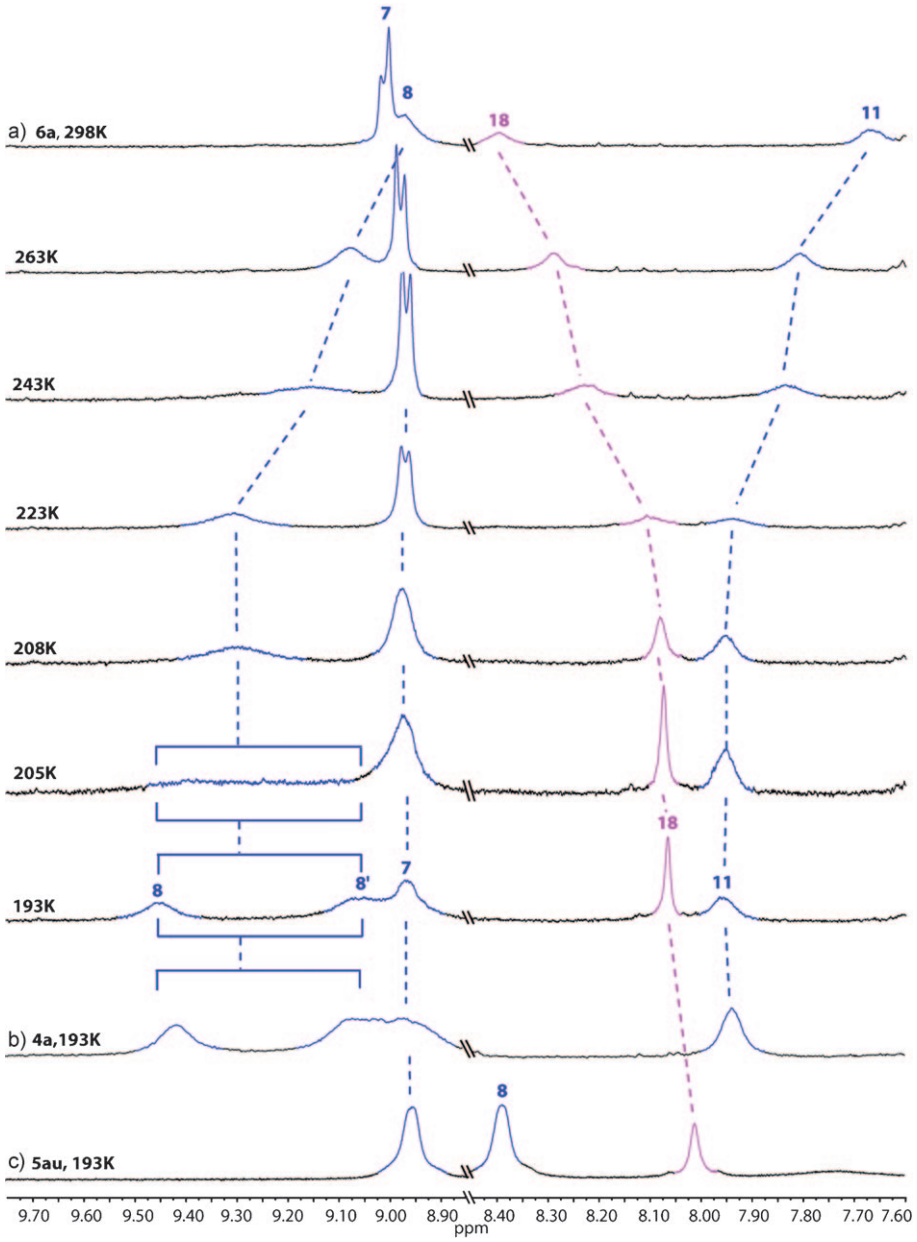

Figure 4. Partial variable-temperature ^{1}H NMR spectra in CD_2Cl_2 of a) oscillating rotaxane **6a**, b) rotaxane **4a** at 193 K, and c) uncomplexed thread **5au** at 193 K.

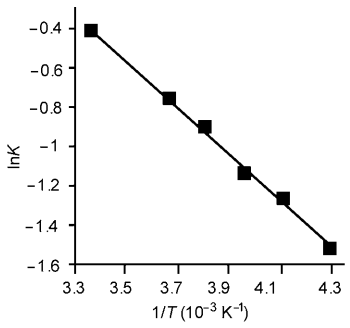

Figure 5. Thermodynamic Van't Hoff plot for exchange between $\mathbf{6a_1}$ and $\mathbf{6a_2}$ in CD_2Cl_2 (233–298 K).

change on the NMR timescale, p_1 and p_2 are the fractional populations of translational isomers $\mathbf{6a_1}$ and $\mathbf{6a_2}$, $\delta\nu$ the difference of resonance of the considered hydrogen atoms when entirely H-bound with DB24C8 and when free. Rate constants k_2 were found to be higher than k_1 at each considered temperature. Arrhenius plots[21] involving kinetic rates k_i based on ^{1}H NMR signal H^{18} (Figure 6a, solid straight line) were linear over the examined temperature range (233–263 K) with a linear regression coefficients of $R_2=$ 0.995 and 0.990. They afforded the energies of activation and the frequency factors for $\mathbf{6a_1}$ of $E_{a1}=34.6$ kJ mol^{-1}, $k_\infty=$ 26226 MHz, and for $\mathbf{6a_2}$ of $E_{a2}=24.4$ kJ mol^{-1}, $k_\infty=$ 611 MHz. Similar data were obtained from H^8-based Arrhenius plots (linear regression coefficients $R_2=0.993$ and 0.978), $E_{a1}=37.1$ kJ mol^{-1}, $k_\infty=$ 111914 MHz for $\mathbf{6a_1}$ and $E_{a2}=$ 26.9 kJ mol^{-1}, $k_\infty=2608$ MHz for $\mathbf{6a_2}$ (Figure 6a, dashed straight line). Furthermore, the activation enthalpies $\Delta H_1^{\neq}=$ 32.6 kJ mol^{-1} for $\mathbf{6a_1}$, $\Delta H_2^{\neq}=$ 22.3 kJ mol^{-1} for $\mathbf{6a_2}$, and entropies $\Delta S_1^{\neq}=-52.2$ J mol^{-1} K^{-1} for $\mathbf{6a_1}$, $\Delta S_2^{\neq}=-83.5$ J mol^{-1} K^{-1} for $\mathbf{6a_2}$ were extracted from the H^{18}-based Eyring plots (linear regression coefficients $R_2=$ 0.993 and 0.978) (Figure 6b, solid straight line).[22] Similar activation enthalpies $\Delta H_1^{\neq}=$ 35.1 kJ mol^{-1} for $\mathbf{6a_1}$, $\Delta H_2^{\neq}=$ 24.9 kJ mol^{-1} for $\mathbf{6a_2}$, and entropies $\Delta S_1^{\neq}=-40.2$ J mol^{-1} K^{-1} for $\mathbf{6a_1}$, $\Delta S_2^{\neq}=-71.4$ J mol^{-1} K^{-1} for $\mathbf{6a_2}$ were extracted from the H^8-based Eyring plots (linear regression coefficients $R_2=0.992$ and 0.974; Figure 6b, dashed straight line). The high negative activation entropies $\Delta S_1^{\neq}$ and $\Delta S_2^{\neq}$ indicate a highly ordered transition state. By comparing $\Delta S^{\neq}$, the higher value observed for $\Delta S_2^{\neq}$ corroborates the better-ordered complex DB24C8/pyridinium amide rather than triazolium/DB24C8.

Free enthalpies of activation $\Delta G_1^{\neq}$ (from $\mathbf{6a_1}$), $\Delta G_2^{\neq}$ (from $\mathbf{6a_2}$), and hence ΔG for the exchange between translational isomers $\mathbf{6a_1}$ and $\mathbf{6a_2}$, were calculated for each temperature in the range of 193–298 K (Figure 7, Table 2). All calculated

 © 2010 Wiley-VCH Verlag GmbH & Co. KGaA, Weinheim

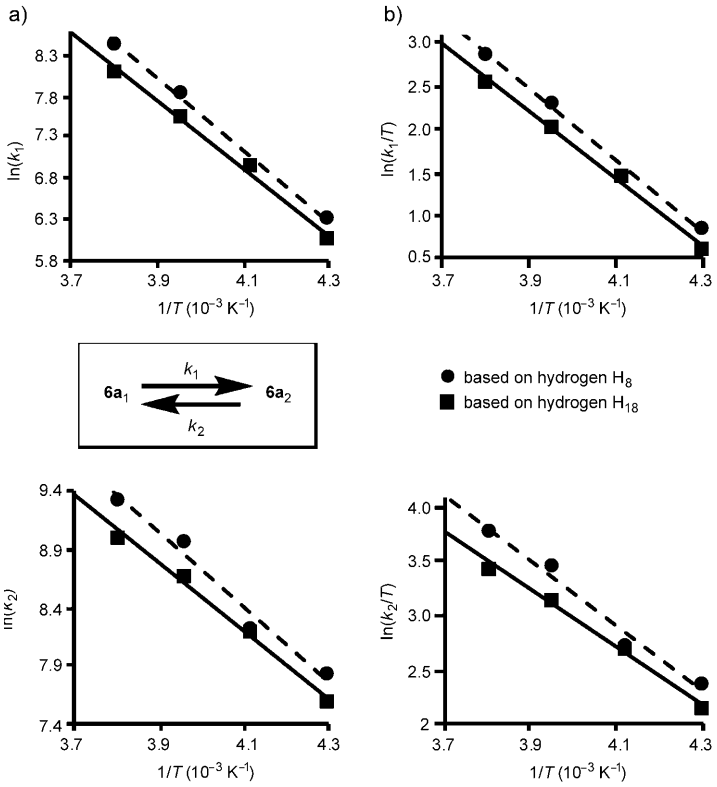

Figure 6. Kinetic plots for exchange in CD_2Cl_2 (233–263 K) between $\mathbf{6a_1}$ and $\mathbf{6a_2}$: a) Arrhenius plots, and (b) Eyring plots.

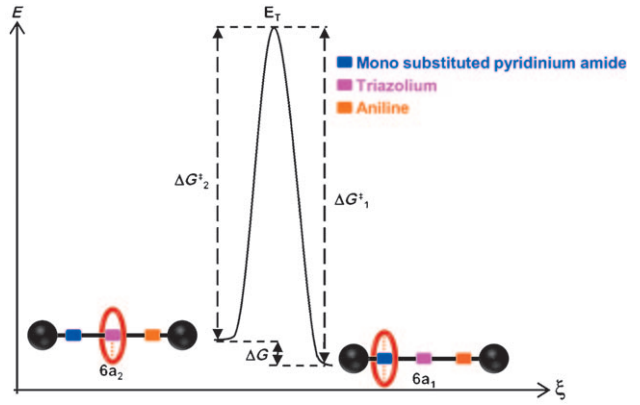

Figure 7. Schematic energetic diagram representation of the translational isomerism between $\mathbf{6a_1}$ and $\mathbf{6a_2}$.

free enthalpies of shuttling exchange ΔG resulting from kinetic parameters k_i match very well with ΔG obtained from thermodynamic parameters K.[23]

In rotaxane **6a**, the covalent bond C^9–C^{10} between the pyridinium and the amide carbonyl group of the monosubstituted pyridinium amide molecular station is frozen in CD_2Cl_2 at low temperature. A single resonance frequency was observed for the two H^8 atoms between 298 and 208 K, which coalesce at 205 K and split at lower temperature (Figure 4, Table 1). Remarkably, no coalescence of H^8 was

Table 2. Free enthalpies of activation $\Delta G_i^{\ddagger}$ and free enthalpies of translational exchange ΔG between $\mathbf{6a_1}$ and $\mathbf{6a_2}$ calculated from kinetic and thermodynamic parameters at various temperatures. All values in kJ mol^{-1}

T [K]	$\Delta G_1^{\ddagger[a]}$	$\Delta G_1^{\ddagger[b]}$	$\Delta G_2^{\ddagger[a]}$	$\Delta G_2^{\ddagger[b]}$	$\Delta G^{[a]}$	$\Delta G^{[b]}$	$\Delta G^{[c]}$
298	48.2	47.0	47.2	46.1	1.0	0.9	1.0
273	46.9	46.0	45.1	44.3	1.8	1.7	1.7
263	46.3	45.6	44.3	43.6	2.0	2.0	2.0
253	45.8	45.2	43.4	42.9	2.4	2.3	2.3
243	45.3	44.8	42.6	42.2	2.7	2.6	2.6
233	44.8	44.4	41.8	41.5	3.0	2.9	2.9
223	44.2	44.0	40.9	40.8	3.3	3.2	3.2
193	42.7	42.8	38.4	38.7	4.3	4.1	4.1

[a,b] Calculated from kinetic parameters based on line broadening of the triazolium H^{18} and pyridinium H^8 signals, respectively. [c] Calculated from thermodynamic parameters.

noticed in thread **5au** or rotaxane **4b** whatever the temperature, that is, DB24C8 acts as a molecular brake of C^9–C^{10} bond rotation only when it is located around both the pyridinium and the monosubstituted amide hydrogen atoms (Figure 8). The observed decrease of the rotation rate in **6a**

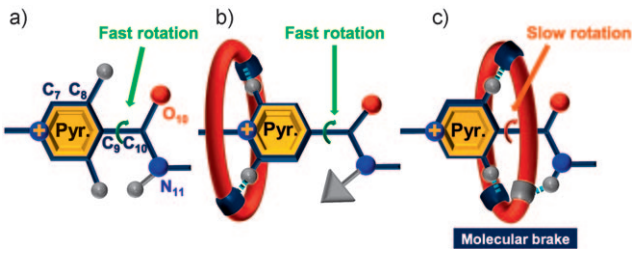

Figure 8. Schematic representation of the role of DB24C8 as a molecular brake for rotation of the C^9–C^{10} bond in a) **5au**, b) **4b**, and c) **4a** and **6a**.

can be explained by anchoring of the macrocycle at the two H-bonding sites surrounding the C^9–C^{10} linkage, which disturbs rotation of the covalent bond (Scheme 4). A very similar coalescence temperature of 203 K was found for H^8 of two-station rotaxane **4a**, which is entirely consistent with the almost quantitative thermodynamic constant K calculated for exchange between $\mathbf{6a_1}$ and $\mathbf{6a_2}$ at 205 K. The equation at the coalescence temperature,[24] $k=\pi\delta\nu/\sqrt{2}$ (where the line widths at half-height of coalesced H^8 correspond to $\delta\nu_c=195$ and 155 Hz for **6a** and **4a**, respectively) afforded rate constants k_{rot} of 433 s^{-1} for **6a** at 205 K and 344 s^{-1} for **4a** at 203 K. Kinetic rates of rotation gave identical free energies of activation of $\Delta G^{\ddagger}_{rot\,205}=39.2$ kJ mol^{-1} for **6a** and $\Delta G^{\ddagger}_{rot\,203}=39.2$ kJ mol^{-1} for **4a**.[25] At a lower temperature of 193 K, H^8 of each rotamer of **4a** and **6a** are split as a result of a slow rotational exchange on the NMR timescale. At this temperature, the equation $k=\pi\Delta\nu$ (where $\Delta\nu=13.6$ and 14 Hz are the extra line broadenings of H^8 for **6a** and **4a**, respectively)[26] provided very similar kinetic rates k_{rot} of 43 s^{-1} for **6a** and 44 s^{-1} for **4a**, which correspond for both rotaxanes to a free energy of activation $\Delta G^{\ddagger}_{rot\,193}$ of 40.5 kJ mol^{-1}.

© 2010 Wiley-VCH Verlag GmbH & Co. KGaA, Weinheim

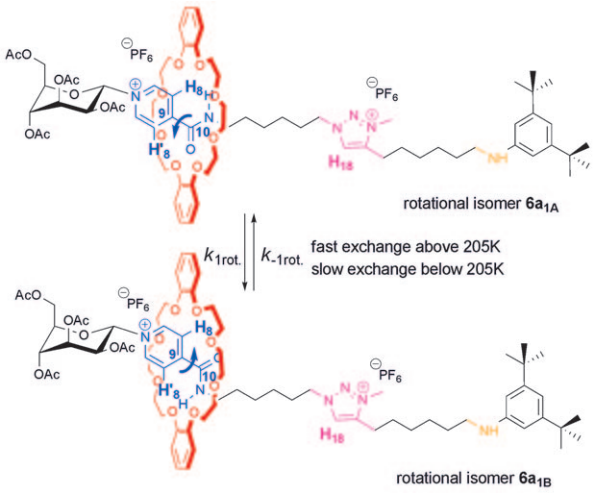

Scheme 4. Exchange between the two rotational isomers **6a$_{1A}$** and **6a$_{1B}$** of rotaxane **6a**.

Conclusion

We have prepared two new rotaxane molecular machines containing three different stations for DB24C8. Variations in pH allow one to determine the following order of affinity of the stations for DB24C8 at room temperature: anilinium > monosubstituted pyridinium amide ≈ triazolium > disubstituted pyridinium amide > aniline. Although the macrocycle resides around the best anilinium station at acidic pH (**5a** and **5b**), the two molecular shuttles **5a**/**6a** and **5b**/**6b** behave very differently upon deprotonation. Disubstituted pyridinium amide containing rotaxanes **5b** and **6b** behave as pH-sensitive bistable rotaxane molecular machines in which DB24C8 is exclusively located around either the anilinium or the triazolium station depending on pH. On the contrary, in deprotonated rotaxane **6a** containing triazolium and monosubstituted pyridinium amide stations, DB24C8 continuously oscillates between the two stations with a very faint preference for the monopyridinium amide station at room temperature. Kinetic and thermodynamic studies demonstrated that the two translational isomers have very similar free enthalpy at room temperature. However, lowering the temperature increases ΔG, and thus forces DB24C8 to reside more and more around the energetically favorable pyridinium amide station. Around 223 K, the oscillation between the two stations stops and DB24C8 spends most of its time around the monosubstituted pyridinium amide station, like in a bistable molecular machine. Increasing the temperature restores the oscillating movement of DB24C8 again, whereas reprotonation of the anilinium moiety turns off the translational oscillation and forces DB24C8 to sit exclusively on the anilinium station. In addition, H-bonding interactions between DB24C8 and the monopyridinium amide station in the deprotonated rotaxane perturb rotation of the threaded pyridinium amide bond, that is, DB24C8 acts as a molecular brake.

Experimental Section

General: All reactions were carried out under an atmosphere of argon unless otherwise indicated. All reagents were purchased from Aldrich and Senn Chemical and were used as received without further purification. Preparation and characterization of threads **5au**, **5bu**, **6au**, and **6bu** are described in the Supporting Information. Dichloromethane was distilled over P_2O_5 and was degassed by bubbling Ar for 20 min. Analytical thin-layer chromatography (TLC) was performed on Merck silica gel 60 F254 plates. Compounds were visualized by dipping the plates in an ethanolic solution of 10% sulfuric acid, ninhydrin, or an aqueous solution of $KMNO_4$, followed by heating. ^{1}H NMR (298 K and variable temperature) and ^{13}C NMR spectra (298 K) were obtained on a Bruker DRX-400 spectrometer (respectively at 400.13 MHz and 100.62 MHz). Chemical shifts are given in ppm with CH_2Cl_2, $CHCl_3$, and CH_3CN as references (δ = 5.32, 7.27, and 1.94 ppm, respectively, for ^{1}H, and δ = 54, 77, 118.26 ppm, respectively, for ^{13}C). Mass spectra (MS) and high-resolution mass spectra (HRMS) were recorded on a ZQ Micromass and Q-TOF Micro (Waters) instruments, respectively.

Rotaxane 3a: $[Cu(CH_3CN)_4]PF_6$ (238 mg, 0.63 mmol, 1 equiv) and 2,6-lutidine (7 μL, 0.06 mmol, 0.1 equiv) were successively added to a solution of **1a** (461 mg, 0.63 mmol, 1 equiv), **2** (293 mg, 0.63 mmol, 1 equiv), and DB24C8 (571 mg, 1.27 mmol, 2 equiv) in dry CH_2Cl_2 (3 mL). The mixture was stirred at room temperature for 24 h then the solvent was removed in vacuo. The crude product was directly purified by chromatography on a silica gel column (solvent gradient elution: CH_2Cl_2, then 25/75 acetone/CH_2Cl_2) to obtain rotaxane **3a** (783 mg, 75%) as a slightly yellow solid. M.p. 78–85 °C; R_f (SiO_2) = 0.62 (40/60 acetone/CH_2Cl_2); ^{1}H NMR (400 MHz, CD_3CN, 298 K): δ = 9.04 (d, 2H, $^3J_{H7\text{-}H8}$ = 6.9 Hz, H^7), 8.60–8.42 (brs, 2H, H^{26}), 8.35 (d, 2H, $^3J_{H8\text{-}H7}$ = 6.9 Hz, H^8), 7.64 (brt, 1H, H^{11}), 7.41 (s, 1H, H^{18}), 7.39 (t, 1H, $^4J_{H30\text{-}H28}$ = 1.6 Hz, H^{30}), 7.33 (d, 2H, $^4J_{H28\text{-}H30}$ = 1.6 Hz, H^{28}), 6.91–6.80 (m, 8H, H$_A$, H$_B$), 6.37 (d, 1H, $^3J_{H1\text{-}H2}$ = 9.0 Hz, H^1), 5.56 (t, 1H, $^3J_{H3\text{-}H2}$ = $^3J_{H3\text{-}H4}$ = 3.4 Hz, H^3), 5.22 (dd, 1H, $^3J_{H2\text{-}H1}$ = 9.0 Hz, $^3J_{H2\text{-}H3}$ = 3.4 Hz, H^2), 5.10 (dd, 1H, $^3J_{H4\text{-}H3}$ = 3.4 Hz, $^3J_{H4\text{-}H5}$ = 2.1 Hz, H^4), 4.81 (dd, 1H, $^3J_{H6a\text{-}H6b}$ = 12.7 Hz, $^3J_{H6a\text{-}H5}$ = 9.2 Hz, H^{6a}), 4.61–4.54 (m, 1H, H^5), 4.31–4.25 (m, 3H, H^{17}, H^{6b}), 4.19–4.05 (m, 10H, H$_C$ H^{25}), 3.84–3.72 (m, 8H, H$_D$), 3.65- 3.58 (m, 4H, H$_E$), 3.44–3.36 (m, 6H, H$_{E'}$, H^{12}), 2.46 (t, 2H, $^3J_{H20\text{-}H21}$ = 7.6 Hz, H^{20}), 2.20 & 2.16 & 2.00 & 1.87 (4s, 12H, CH_3CO), 1.86–1.80 (m, 2H, H^{16}), 1.67–1.56 (m, 4H, H^{13}, H^{24}), 1.45–1.27 (m, 6H, H^{14}, H^{15}, H^{21}), 1.25–1.10 (m, 4H, H^{22}, H^{23}), 1.18 ppm (s, 18H, H^{32}); ^{13}C NMR (100 MHz, CD_3CN, 298 K): δ = 171.5 & 170.3 & 170.0 & 169.9 ($COCH_3$), 162.4 (C^{10}), 153.6 (C^{29}), 153.0 (C^9), 148.4 (C^{19}), 148.3 (C$_q$ DB24C8), 144.1 (C^7), 136.1 (C^{27}), 127.2 (C^8), 124.9 (C^{30}), 122.1 & 113.2 (C$_A$, C$_B$), 122.0 (C^{18}), 117.8 (C^{28}), 89.1 (C^1), 78.6 (C^5), 71.6 (C$_E$), 71.0 (C$_D$), 69.6 (C^2), 69.1 (C$_C$), 68.3 (C^4), 67.4 (C^3), 60.9 (C^6), 51.6 (C^{25}), 50.4 (C^{17}), 40.9 (C^{12}), 35.6 (C^{31}), 31.4 (C^{32}), 30.8 (C^{16}), 29.9 & 29.4 & 29.4 & 28.2 & 26.7 & 26.6 & 26.4 (C^{13}, C^{14}, C^{15}, C^{21} C^{22}, C^{23}, C^{24}), 25.9 (C^{20}), 21.0 & 20.9 & 20.8 & 20.4 ppm (CH_3CO); HRMS (ESI): $[M-2PF_6]^{2+}$ calcd for $C_{72}H_{104}N_6O_{18}^{2+}$: 670.3704, found: 670.3683.

Rotaxane 3b: $[Cu(CH_3CN)_4]PF_6$ (81 mg, 0.22 mmol, 1 equiv) and 2,6-lutidine (2.5 μL, 0.02 mmol, 0.1 equiv) were added successively to a solution of mannosyl azide **1b** (160 mg, 0.22 mmol, 1 equiv), alkyne **2** (100 mg, 0.22 mmol, 1 equiv), and DB24C8 (194 mg, 0.44 mmol, 2 equiv) in dry CH_2Cl_2 (3 mL). The mixture was stirred for 24 h at room temperature, and then the solvent was removed in vacuo. The crude product was directly purified by column chromatography (SiO_2: solvent gradient elution: acetone/CH_2Cl_2 20/80, then 30/70) to afford pure rotaxane **3b** (266 mg, 74%) as a white solid. M.p. 97–105 °C; R_f (SiO_2) = 0.30 (30/70 acetone/CH_2Cl_2); ratio of isomers: 50/50; ^{1}H NMR (400 MHz, CD_3CN, 298 K): δ = 8.99 & 8.98 (2d, 2H, $^3J_{H7\text{-}H8}$ = 6.9 Hz, H^7), 8.59–8.43 (brs, 2H, H^{26}), 8.07 & 8.04 (2d, 2H, $^3J_{H8\text{-}H7}$ = 6.9 Hz, H^8), 7.43 & 7.40 (2s, 1H, H^{18}), 7.41–7.38 (brs, 1H, H^{30}), 7.34 (d, 2H, $^4J_{H28\text{-}H30}$ = 1.5 Hz, H^{28}), 6.91–6.80 (m, 8H, H$_A$ H$_B$), 6.36 & 6.33 (2d, 1H, $^3J_{H1\text{-}H2}$ = 9.4 Hz, H^1), 5.57 (brt, 1H, H^3), 5.25 & 5.23 (2dd, 1H, $^3J_{H2\text{-}H1}$ = 9.3 Hz, $^3J_{H2\text{-}H3}$ = 3.2 Hz, H^2), 5.11 (brt, 1H, H^4), 4.79 & 4.76 (2dd, 1H, $^2J_{H6a\text{-}H6b}$ = 12.8 Hz, $^3J_{H6a\text{-}H5}$ = 9.0 Hz, H^{6a}), 4.59–4.54 (m, 1H, H^5), 4.33–4.26 (m, 1H, H^{6b}), 4.29 & 4.22 (2t, 2H, $^3J_{H17\text{-}H16}$ = 7.1 Hz, H^{17}), 4.19–4.05 (m, 10H, H$_C$ H^{25}), 3.85–3.72 (m, 8H, H$_D$), 3.65–3.58 (m, 4H, H$_E$), 3.49 & 3.08 (2t, 2H, $^3J_{H12\text{-}H13}$ = 7.4 Hz, H^{12}), 3.45–

© 2010 Wiley-VCH Verlag GmbH & Co. KGaA, Weinheim

3.38 (m, 4H, $H_{E'}$), 3.03 & 2.84 (2 s, 3H, H^{11}), 2.47 & 2.46 (2t, 2H, $^3J_{H20\text{-}H21}$ = 7.8 Hz, H^{20}), 2.20 & 2.20 & 2.15 & 2.14 & 2.01 & 2.00 & 1.90 (7 s, 12H, CH_3CO), 1.92–1.83 & 1.82–1.72 (2 m, 2H, H^{16}), 1.69–1.49 (m, 4H, H^{13} H^{24}), 1.44–1.13 (m, 10H, H^{14} H^{15} H^{21} H^{22} H^{23}), 1.19 ppm (s, 18H, H^{32}); ^{13}C NMR (100 MHz, CD_3CN, 298 K): δ = 171.5 & 171.5 & 170.3 & 170.1 & 170.0 & 170.0 ($COCH_3$), 165.7 & 165.6 (C^{10}), 156.6 & 156.5 (C^9), 153.6 & 148.4 (C^{19} C^{29}), 144.1 & 144.0 (C^7), 136.1 (C^{27}), 127.1 & 126.8 (C^8), 124.8 (C^{30}), 122.2 & 113.3 (C_A, C_B), 122.0 (C^{18}), 117.8 (C^{28}), 89.2 & 89.1 (C^1), 78.4 & 78.3 (C^5), 71.6 (C_E), 71.0 (C_D), 69.7 & 69.6 (C^2), 69.1 (C_C), 68.3 (C^4), 67.6 & 67.5 (C^3), 61.1 & 61.0 (C^6), 51.6 (C^{25}), 51.2 & 47.9 (C^{12}), 50.5 & 50.4 (C^{17}), 37.0 & 32.7 (C^{11}), 35.6 (C^{31}), 31.4 (C^{32}), 30.8 & 30.6 & 29.9 & 29.9 & 29.4 & 29.4 & 28.3 & 28.2 & 27.1 & 26.8 & 26.7 & 26.6 & 26.4 & 26.4 & 26.2 (C^{13}, C^{14}, C^{15}, C^{16}, C^{21}, C^{22}, C^{23}, C^{24}), 25.9 & 25.9 (C^{20}), 21.0 & 20.9 & 20.8 & 20.5 & 20.5 ppm (CH_3CO); HRMS (ESI): $[M-2PF_6]^{2+}$ calcd for $C_{73}H_{106}N_6O_{18}^{2+}$: 677.3782, found: 677.3755.

Rotaxane 4a: An excess of DIEA (5 equiv) was added to a solution of rotaxane **3a** in CD_3CN to give the deprotonated rotaxane **4a**. R_f (SiO_2) = 0.40 (30/70 acetone/CH_2Cl_2); ^{1}H NMR (400 MHz, CD_3CN, 298 K): δ = 9.31 (d, 2H, $^3J_{H8\text{-}H7}$ = 6.8 Hz, H^8), 8.99 (d, 2H, $^3J_{H7\text{-}H8}$ = 6.8 Hz, H^7), 7.98 (brt, 1H, H^{11}), 7.46 (s, 1H, H^{18}), 7.01–6.92 (m, 8H, H_A H_B), 6.72 (t, 1H, $^4J_{H30\text{-}H28}$ = 1.6 Hz, H^{30}), 6.45 (d, 2H, $^4J_{H28\text{-}H30}$ = 1.6 Hz, H^{28}), 6.33 (d, 1H, $^3J_{H1\text{-}H2}$ = 9.1 Hz, H^1), 5.45 (t, 1H, $^3J_{H3\text{-}H2}$ = $^3J_{H3\text{-}H4}$ = 3.4 Hz, H^3), 5.26 (dd, 1H, $^3J_{H2\text{-}H1}$ = 9.1 Hz, $^3J_{H2\text{-}H3}$ = 3.4 Hz, H^2), 4.99 (dd, 1H, $^3J_{H4\text{-}H3}$ = 3.4 Hz, $^3J_{H4\text{-}H5}$ = 1.8 Hz, H^4), 4.95 (dd, 1H, $^2J_{H6a\text{-}H6b}$ = 12.9 Hz, $^3J_{H6a\text{-}H5}$ = 9.7 Hz, H^{6a}), 4.38–4.32 (m, 1H, H^5), 4.19 (t, 2H, $^3J_{H17\text{-}H16}$ = 7.0 Hz, H^{17}), 4.14–4.06 (m, 8H, H_C), 4.05 (dd, 1H, $^3J_{H6b\text{-}H6a}$ = 12.9 Hz, $^3J_{H6b\text{-}H5}$ = 3.4 Hz, H^{6b}), 3.67–3.53 (m, 8H, H_D), 3.20–3.02 (m, 8H, H_E H^{12} H^{25}), 2.69–2.60 (m, 6H, $H_{E'}$, H^{20}), 2.12 & 2.00 & 1.96 & 1.84 (4 s, 12H, CH_3CO), 1.70–1.61 (m, 4H, H^{16}, H^{21}), 1.60–1.52 (m, 2H, H^{24}), 1.46–1.34 (m, 4H, H^{23}, H^{22}), 1.25 (s, 18H, H^{32}), 1.15–1.08 (m, 4H, H^{13}, H^{14}), 1.08–0.99 ppm (m, 2H, H^{15}); ^{13}C NMR (100 MHz, CD_3CN, 298 K): δ = 171.7 & 170.2 & 170.0 & 169.8 ($COCH_3$), 163.0 (C^{10}), 152.5 & 152.3 & 149.6 (C^9 C^{27}, C^{29}), 149.6 (C^{19}), 148.6 (C_q DB24C8), 142.8 (C^7), 130.1 (C^8), 122.1 & 112.8 & 112.7 (C_A, C_B), 122.0 (C^{18}), 111.8 (C^{30}), 108.0 (C^{28}), 88.6 (C^1), 78.9 (C^5), 70.4 (C_E), 70.3 (C_D), 69.0 (C_C), 68.9 (C^2), 68.1 (C^4), 67.3 (C^3), 60.3 (C^6), 50.4 (C^{17}), 44.3 (C^{25}), 40.7 (C^{12}), 35.3 (C^{31}), 31.6 (C^{32}), 30.7 & 30.2 & 29.9 & 29.5 & 29.3 & 27.5 & 26.5 & 26.0 (C^{13}, C^{14}, C^{15}, C^{16}, C^{21}, C^{22}, C^{23}, C^{24}), 21.0 & 20.9 & 20.8 & 20.7 ppm (CH_3CO); HRMS (ESI): $[M-PF_6+H]^{2+}$ calcd for $C_{72}H_{104}N_6O_{18}^{2+}$: 670.3704, found: 670.3704.

Rotaxane 4b: An excess of DIEA (5 equiv) was added to a solution of rotaxane **3b** in CD_3CN to give deprotonated rotaxane **4b**. R_f (SiO_2) = 0.37 (30/70 acetone/CH_2Cl_2); ratio of isomers: 50/50; ^{1}H NMR (400 MHz, CD_3CN, 298 K): δ = 9.97 & 9.92 (d & brd, 2H, $^3J_{H7\text{-}H8}$ = 6.6 Hz, H^7), 8.06 & 8.02 (2d, 2H, $^3J_{H8'\text{-}H7'}$ = 6.7 Hz & $^3J_{H8\text{-}H7}$ = 6.6 Hz, H^8), 7.49 & 7.46 (2 s, 1H, H^{18}), 7.02–6.87 (m, 8H, H_A H_B), 6.73–6.70 (brs, 1H, H^{30}), 6.45 (d, 2H, $^4J_{H28\text{-}H30}$ = 1.4 Hz, H^{28}), 6.35 & 6.34 (d & brd, 1H, $^3J_{H1'\text{-}H2'}$ = 2.3 Hz & $^3J_{H1\text{-}H2}$ = 3.0 Hz, H^1), 5.96 & 5.94–5.90 (t & m, 1H, $^3J_{H2\text{-}H1}$ = $^3J_{H2\text{-}H3}$ = 3.0 Hz, H^2), 5.46–5.39 (m, 1H, H^3), 5.15 (t, 1H, $^3J_{H4\text{-}H3}$ = $^3J_{H4\text{-}H5}$ = 8.4 Hz, H^4), 4.37–4.20 (m, 5H, H^5, H^{17} H_C), 4.20–4.05 (m, 4H, H^{6a}, H^{6b}, H_C), 4.05–3.89 (m, 4H, H_C), 3.77–3.63 (m, 4H, H_D), 3.63–3.51 (m, 4H, $H_{D'}$), 3.50–3.39 (m, 5H, H_E, $H_{12'}$), 3.20–3.03 (m, 7H, H^{12}, H^{25}, $H_{E'}$), 3.01 & 2.85 (2 s, 3H, H^{11}), 2.64 (t, 2H, $^3J_{H20\text{-}H21}$ = 7.5 Hz, H^{20}), 1.97–1.70 (m, 2H, H^{16}), 1.94 & 1.82 & 1.81 & 1.77 & 1.75 (5 s, 12H, CH_3CO), 1.68–1.47 (m, 6H, H^{13}, H^{21}, H^{24}), 1.47–1.34 (m, 4H, H^{22}, H^{23}), 1.33–1.16 (m, 4H, H^{14}, H^{15}), 1.26 ppm (s, 18H, H^{32}); ^{13}C NMR (100 MHz, CD_3CN, 298 K): δ = 171.1 & 171.0 & 170.3 & 169.9 & 169.8 & 169.8 & 169.7 ($COCH_3$), 166.8 (C^{10}), 153.6 & 149.6 (C^9, C^{27}), 152.3 & 148.5 & 148.4 (C^{19}, C^{29}), 147.8 & 147.6 (C^7), 125.4 & 124.9 (C^8), 122.3 (C^{18}), 122.2 & 122.1 & 113.3 & 113.2 & 113.1 & 113.0 (C_A, C_B), 111.8 (C^{30}), 108.0 (C^{28}), 93.5 & 93.2 (C^1), 74.0 & 73.8 (C^5), 72.8 & 72.7 & 72.6 & 72.6 (C_E), 71.5 & 71.3 & 71.2 (C_D), 69.4 & 69.3 & 69.2 & 69.2 (C_C), 68.9 & 68.8 & 68.7 (C^2, C^3), 66.6 & 66.5 (C^4), 61.6 (C^6), 51.4 & 47.6 (C^{12}), 50.4 & 50.4 (C^{17}) , 44.4 (C^{25}), 37.1 & 32.6 (C^{11}), 35.3 (C^{31}), 31.6 (C^{32}), 30.7 & 30.1 & 30.1 & 30.0 & 29.6 & 29.5 & 28.6 & 27.5 & 27.0 & 26.9 & 26.7 & 26.7 & 26.6 (C^{13}, C^{14}, C^{15}, C^{16}, C^{21}, C^{22}, C^{23}, C^{24}), 26.0 (C^{20}), 20.7 & 20.6 & 20.5 & 19.6 ppm (CH_3CO); HRMS (ESI): $[M-PF_6+H]^{2+}$ calcd for $C_{73}H_{106}N_6O_{18}^{2+}$: 677.3782, found: 677.3781.

Rotaxane 5a. Rotaxane **3a** (98 mg, 0.06 mmol, 1 equiv) was dissolved in iodomethane (1 mL) and the mixture stirred for three days at room temperature. After removing iodomethane in vacuo, the yellow powder was washed with Et_2O to afford the pure methylated triazolium iodide product (106 mg, quantitative). This material (106 mg, 0.06 mmol, 1 equiv) was dissolved in CH_2Cl_2 (5 mL) and added to a solution of NH_4PF_6 (49 mg, 0.30 mmol, 5 equiv) in MilliQ water (5 mL). The biphasic solution was vigorously stirred for 30 min at RT. After separation, the aqueous layer was extracted with CH_2Cl_2 (2 × 5 mL). The organic layers were combined, dried over $MgSO_4$, and concentrated to give rotaxane **4a** (99 mg, 93 %) as a yellow oil. R_f (SiO_2) = 0.5 (30/70 acetone/CH_2Cl_2); ^{1}H NMR (400 MHz, CD_3CN, 298 K): δ = 9.05 (d, 2H, $^3J_{H7\text{-}H8}$ = 6.9 Hz, H^7), 8.61–8.49 (2H, brs, H^{26}), 8.35 (2H, d, $^3J_{H8\text{-}H7}$ = 6.9 Hz, H^8), 8.01 (1H, s, H^{18}), 7.61 (brt, 1H, $^3J_{H11\text{-}H12}$ = 7.0 Hz, H^{11}), 7.42 (t, 1H, $^4J_{H30\text{-}H28}$ = 1.6 Hz, H^{30}), 7.34 (d, 2H, $^4J_{H28\text{-}H30}$ = 1.6 Hz, H^{28}), 6.93–6.82 (m, 8H, H_A H_B), 6.38 (d, 1H, $^3J_{H1\text{-}H2}$ = 9.1 Hz, H^1), 5.57 (t, 1H, $^3J_{H3\text{-}H2}$ = $^3J_{H3\text{-}H4}$ = 3.4 Hz, H^3), 5.22 (dd, 1H, $^3J_{H2\text{-}H1}$ = 9.1 Hz, $^3J_{H2\text{-}H3}$ = 3.4 Hz, H^2), 5.10 (dd, 1H, $^3J_{H4\text{-}H3}$ = 3.4 Hz, $^3J_{H4\text{-}H5}$ = 2.0 Hz, H^4), 4.82 (dd, 1H, $^2J_{H6a\text{-}H6b}$ = 12.7 Hz, $^3J_{H6a\text{-}H5}$ = 9.2 Hz, H^{6a}), 4.58 (ddd, 1H, $^3J_{H5\text{-}H6a}$ = 9.2 Hz, $^3J_{H5\text{-}H6b}$ = 3.8 Hz, $^3J_{H5\text{-}H4}$ = 2.0 Hz, H^5), 4.49 (t, 2H, $^3J_{H17\text{-}H16}$ = 7.2 Hz, H^{17}), 4.29 (dd, 1H, $^2J_{H6b\text{-}H6a}$ = 12.7 Hz, $^3J_{H6b\text{-}H5}$ = 3.8 Hz, H^{6b}), 4.21–4.07 (m, 10H, H^{25}, H_C), 4.04 (s, 3H, H^{33}), 3.86–3.74 (m, 8H, H_D), 3.66–3.60 (m, 4H, H_E), 3.45–3.37 (m, 6H, H^{12}, $H_{E'}$), 2.51 (t, 2H, $^3J_{H20\text{-}H21}$ = 7.6 Hz, H^{20}), 2.21 & 2.16 & 2.00 & 1.86 (4 s, 12H, CH_3CO), 1.99–1.94 (m, 2H, H^{16}), 1.72–1.59 (m, 4H, H^{13}, H^{24}), 1.47–1.31 (m, 6H, H^{14}, H^{15}, H^{21}), 1.30–1.16 (m, 4H, H^{22}, H^{23}), 1.19 ppm (s, 18H, H^{32}); ^{13}C NMR (100 MHz, CD_3CN, 298 K): δ = 171.5 & 170.3 & 170.0 & 169.9 ($COCH_3$), 162.5 (C^{10}), 153.7 (C^{29}), 153.0 (C^9), 148.4 (C_q DB24C8), 145.5 (C^{19}), 144.1 (C^7), 136.1 (C^{27}), 128.3 (C^{18}), 127.2 (C^8), 124.9 (C^{30}), 122.2 & 113.3 (C_A, C_B), 117.8 (C^{28}), 89.0 (C^1), 78.6 (C^5), 71.6 (C_E), 71.0 (C_D), 69.6 (C^2), 69.1 (C_C), 68.3 (C^4), 67.4 (C^3), 60.9 (C^6), 54.4 (C^{17}), 51.5 (C^{25}), 40.9 (C^{12}), 38.1 (C^{33}), 35.6 (C^{31}), 31.4 (C^{32}), 29.7 & 29.3 & 29.1 & 28.1 & 27.2 & 26.7 & 26.3 & 26.1 (C^{13}, C^{14}, C^{15}, C^{16}, C^{21}, C^{22}, C^{23}, C^{24}), 23.5 (C^{20}), 21.0 & 20.8 & 20.8 & 20.4 ppm (CH_3CO); HRMS (ESI): $[M-3PF_6]^{3+}$; calcd for $[C_{73}H_{107}N_6O_{18}]^{3+}$: 451.9210, found: 451.9196.

Rotaxane 5b: Rotaxane **3b** (140 mg, 0.085 mmol, 1 equiv) was dissolved in iodomethane (1 mL) and the mixture stirred for 3 d at RT. After removing iodomethane in vacuo, the solid was washed with Et_2O, and then dissolved in CH_2Cl_2 (5 mL). To this solution was added a solution of NH_4PF_6 (69 mg, 0.42 mmol, 5 equiv) in MilliQ water (5 mL). The biphasic solution was vigorously stirred for 30 min at room temperature. After separation, the aqueous layer was extracted with CH_2Cl_2 (2 × 5 mL). The organic layers were combined, dried over $MgSO_4$ and concentrated to give rotaxane **5b** (139 mg, 91 %) as a colorless oil. R_f (SiO_2) = 0.54 (30/70 acetone/CH_2Cl_2); ratio of isomers: 58/42 (*trans*/*cis*); ^{1}H NMR (400 MHz, CD_3CN, 298 K): δ = 8.98 (d, 2H, $^3J_{H7\text{-}H8}$ = 6.7 Hz, H^7), 8.60–8.50 (brs, 2H, H^{26}), 8.06 & 8.05 (2d, 2H, $^3J_{H8\text{-}H7}$ = 6.7 Hz, H^8), 8.01 & 7.99 (2 s, 1H, H^{18}), 7.44–7.40 (brs, 1H, H^{30}), 7.34 (brd, 2H, $^4J_{H28\text{-}H30}$ = 1.3 Hz, H^{28}), 6.93–6.80 (m, 8H, H_A H_B), 6.34 (d, 1H, $^3J_{H1\text{-}H2}$ = 8.7 Hz, H^1), 5.57 (t, 1H, $^3J_{H3\text{-}H2}$ = $^3J_{H3\text{-}H4}$ = 3.5 Hz, H^3), 5.23 & 5.22 (2dd, 1H, $^3J_{H2\text{-}H1}$ = 8.7 Hz, $^3J_{H2\text{-}H3}$ = 3.5 Hz, H^2), 5.13–5.09 (m, 1H, H^4), 4.81 & 4.79 (2dd, 1H, $^2J_{H6a\text{-}H6b}$ = 12.7 Hz, $^3J_{H6a\text{-}H5}$ = 9.1 Hz, H^{6a}), 4.59–4.54 (m, 1H, H^5), 4.50 & 4.44 (t, 2H, $^3J_{H17\text{-}H16}$ = 7.2 Hz, H^{17}), 4.31 & 4.28 (2dd, 1H, $^2J_{H6b\text{-}H6a}$ = 12.7 Hz, $^3J_{H6b\text{-}H5}$ = 4.9 Hz, H^{6b}), 4.21–4.05 (m, 10H, H^{25}, H_C), 4.04 & 4.03 (2 s, 3H, H_{33}), 3.86–3.69 (m, 8H, H_D), 3.67–3.58 (m, 4H, H_E), 3.50 & 3.11 (2t, 2H, $^3J_{H12\text{-}H13}$ = 7.4 Hz, H^{12}), 3.45–3.37 (m, 4H, $H_{E'}$), 3.04 & 2.85 (2 s, 3H, H^{11}), 2.54–2.46 (m, 2H, H^{20}), 2.20 & 2.15 & 2.01 & 1.90 (4 s, 12H, CH_3CO), 2.00–1.86 (m, 2H, H^{16}), 1.73–1.49 (m, 4H, H^{13}, H^{24}), 1.46–1.14 (m, 10H, H^{14}, H^{15}, H^{21}, H^{22}, H^{23}), 1.19 ppm (m, 18H, H^{32}); ^{13}C NMR (100 MHz, CD_3CN, 298 K): δ = 171.5 & 170.3 & 170.0 ($COCH_3$), 165.7 & 165.6 (C^{10}), 156.7 & 156.5 (C^9), 153.7 (C^{29}), 148.4 (C_q DB24C8), 145.5 (C^{19}), 144.1 (C^7), 136.1 (C^{27}), 128.2 (C^{18}), 127.1 & 126.9 (C^8), 125.0 (C^{30}), 122.2 & 113.4 (C_A, C_B), 117.8 (C^{28}), 89.1 (C^1), 78.5 & 78.4 (C^5), 71.6 (C_E), 71.0 (C_D), 69.6 (C^2), 69.1 (C_C), 68.2 (C^4), 67.5 (C^3), 61.0 (C^6), 54.5 & 54.4 (C^{17}), 51.6 (C^{25}), 51.3 & 47.9 (C^{12}), 38.2 (C^{33}), 37.1 & 32.7 (C^{11}), 35.7 (C^{31}), 31.4 (C^{32}), 31.3 & 29.8 & 29.6 & 29.2 & 28.3 & 28.1 & 27.3 & 27.0 & 26.6 & 26.4 & 26.2 (C^{13}, C^{14}, C^{15}, C^{16}, C^{21}, C^{22}, C^{23}, C^{24}), 23.5 (C^{20}), 21.0 & 20.9 & 20.8 & 20.6 & 20.5 ppm (CH_3CO); HRMS (ESI): $[M-3PF_6]^{3+}$ calcd for $[C_{74}H_{109}N_6O_{18}]^{3+}$: 456.5933, found: 456.5919.

 © 2010 Wiley-VCH Verlag GmbH & Co. KGaA, Weinheim

Rotaxane 6a: An excess of DIEA (5 equiv) was added to a solution of rotaxane **5a** in CD_3CN to give deprotonated rotaxane **6a**. ^{1}H NMR (400 MHz, CD_3CN, 298 K): $\delta = 9.01$ (d, 2H, $^3J_{H7\text{-}H8} = 6.8$ Hz, H^7), 8.97–8.90 (m, 2H, H^8), 8.38–8.31 (brs, 1H, H^{18}), 7.82 (brt, 1H, $^3J_{H11\text{-}H12} = 6.9$ Hz, H^{11}), 6.96–6.89 (m, 8H, H_A H_B), 6.73 (t, 1H, $^4J_{H30\text{-}H28} = 1.6$ Hz, H^{30}), 6.46 (d, 2H, $^4J_{H28\text{-}H30} = 1.6$ Hz, H^{28}), 6.35 (d, 1H, $^3J_{H1\text{-}H2} = 9.1$ Hz, H^1), 5.50 (t, 1H, $^3J_{H3\text{-}H1} = {}^3J_{H3\text{-}H4} = 3.4$ Hz, H^3), 5.25 (dd, 1H, $^3J_{H2\text{-}H1} = 9.1$ Hz, $^3J_{H2\text{-}H3} = 3.4$ Hz, H^2), 5.04 (dd, 1H, $^3J_{H4\text{-}H3} = 3.4$ Hz, $^3J_{H4\text{-}H5} = 1.9$ Hz, H^4), 4.90 (dd, 1H, $^2J_{H6a\text{-}H6b} = 12.9$ Hz, $^3J_{H6a\text{-}H5} = 9.5$ Hz, H^{6a}), 4.65–4.55 (m, 2H, H^{17}), 4.42 (ddd, 1H, $^3J_{H5\text{-}H6a} = 9.5$ Hz, $^3J_{H5\text{-}H6b} = 3.6$ Hz, $^3J_{H5\text{-}H4} = 1.9$ Hz, H^5), 4.14 (dd, 1H, $^2J_{H6b\text{-}H6a} = 12.9$ Hz, $^3J_{H6b\text{-}H5} = 3.6$ Hz, H^{6b}), 4.11–4.02 (m, 8H, H_C), 3.89 (s, 3H, H_{33}), 3.71–3.61 (m, 8H, H_D), 3.33–3.23 (m, 4H, H_E), 3.23–3.14 (m, 2H, H^{12}), 3.08 (t, 2H, $^3J_{H25\text{-}H24} = 6.9$ Hz, H^{25}), 3.04–2.94 (m, 4H, $H_{E'}$), 2.62–2.52 (m, 2H, H^{20}), 2.15 & 2.07 & 2.00 & 1.85 (4s, 12H, CH_3CO), 1.98–1.90 (m, 2H, H^{16}), 1.67–1.53 (m, 4H, H^{21}, H^{24}), 1.46–1.35 (m, 4H, H^{22}, H^{23}), 1.30–1.24 (m, 2H, H^{13}), 1.26 (s, 18H, H^{32}), 1.24–1.17 ppm (m, 4H, H^{14} H^{15}); ^{13}C NMR (100 MHz, CD_3CN, 298 K): $\delta =$ 170.3 & 170.0 & 169.9 ($COCH_3$), 162.8 (C^{10}), 156.2 (C^9), 152.3 (C^{29}), 149.6 (C^{27}), 148.6 (C_q DB24C8), 143.4 (C^7), 129.0 (C^8), 122.0 & 112.8 (C_A, C_B), 112.0 (C^{30}), 108.0 (C^{28}), 88.8 (C^1), 78.9 (C^5), 70.9 (C_E), 70.5 (C_D), 69.2 (C^2), 69.0 (C_C), 68.2 (C^4), 67.4 (C^3), 60.6 (C^6), 54.3 (C^{17}), 44.3 (C^{25}), 40.7 (C^{12}), 37.7 (C^{33}), 35.3 (C^{31}), 31.6 (C^{32}), 29.9 & 29.4 & 29.2 & 28.9 & 28.0 & 26.7 & 26.2 (C^{13}, C^{14}, C^{15}, C^{16}, C^{21}, C^{22}, C^{23}, C^{24}), 23.5 (C^{20}), 21.0 & 20.9 & 20.6 & 20.1 ppm (CH_3CO); HRMS (ESI): $[M\text{-}2PF_6]^{2+}$; calcd for $[C_{73}H_{106}N_6O_{18}]^{2+}$: 677.3782, found: 677.3768.

Rotaxane 6b: An excess of DIEA (5 equiv) was added to a solution of rotaxane **5b** in CD_3CN to give the deprotonated rotaxane **6b**. Ratio of isomers: 58/42 (*trans*/*cis*); ^{1}H NMR (400 MHz, CD_3CN, 298 K): $\delta = 8.97$ & 8.96 (2d, 2H, $^3J_{H7\text{-}H8} = 6.7$ Hz, H^7), 8.74 & 8.71 (2s, 1H, H^{18}), 8.03 & 8.00 (2d, 2H, $^3J_{H8\text{-}H7} = 6.7$ Hz, H^8), 6.87–6.79 (m, 8H, H_A H_B), 6.73 (t, 1H, $^4J_{H30\text{-}H28} = 1.6$ Hz, H^{30}), 6.47–6.45 (brs, 2H, H^{28}), 6.35 (d, 1H, $^3J_{H1\text{-}H2} = 8.7$ Hz, H^1), 5.57 (t, 1H, $^3J_{H3\text{-}H5} = {}^3J_{H3\text{-}H4} = 3.4$ Hz, H^3), 5.22 & 5.20 (2dd, 1H, $^3J_{H2\text{-}H1} = 8.7$ Hz, $^3J_{H2\text{-}H3} = 3.4$ Hz, H^2), 5.13–5.09 (m, 1H, H^4), 5.06–4.85 (brs, 2H, H^{17}), 4.81 & 4.80 (2dd, 1H, $^2J_{H6a\text{-}H6b} = 12.8$ Hz, $^3J_{H6a\text{-}H5} = 9.0$ Hz, H^{6a}), 4.59–4.53 (m, 1H, H^5), 4.30 & 4.29 (2dd, 1H, $^2J_{H6b\text{-}H6a} = 12.8$ Hz, $^3J_{H6b\text{-}H5} = 4.3$ Hz, H^{6b}), 4.10–3.97 (m, 8H, H_C), 3.82–3.68 (m, 8H, H_D), 3.67–3.45 (m, 11H, H_{33} H_E), 3.36 & 2.95 (2t, 2H, $^3J_{H12\text{-}H13} = 7.4$ Hz, H^{12}), 3.10–3.03 (m, 2H, H^{25}), 2.97 & 2.79 (2s, 3H, H^{11}), 2.71–2.68 (m, 2H, H^{20}), 2.16 & 2.15 & 2.01 & 1.99 & 1.90 & 1.87 (6s, 12H, CH_3CO), 1.58–1.05 (m, 16H, H^{13}, H^{14}, H^{15}, H^{16}, H^{21}, H^{22}, H^{23}, H^{24}), 1.26 ppm (s, 18H, H^{32}); ^{13}C NMR (100 MHz, CD_3CN, 298 K): $\delta = 170.3$ & 170.3 & 170.1 & 170.0 ($COCH_3$), 165.6 & 165.4 (C^{10}), 156.7 & 156.5 (C^9), 152.4 (C^{29}), 149.6 (C^{27}), 148.7 & 148.6 (C_q DB24C8), 144.1 (C^7), 129.6 (C^{18}), 127.0 & 126.9 (C^8), 121.7 & 112.8 (C_A, C_B), 111.9 (C^{30}), 108.0 (C^{28}), 89.1 (C^1), 78.5 & 78.5 (C^5), 71.8 (C_E), 70.8 (C_D), 69.6 (C^2), 69.0 (C_C), 68.2 (C^4), 67.5 (C^3), 61.0 (C^6), 54.3 (C^{17}), 51.3 & 48.0 (C^{12}), 44.3 (C^{25}), 37.1 & 32.9 (C^{11}), 35.3 (C^{31}), 31.7 (C^{32}), 29.9 & 29.4 & 28.7 & 27.3 & 27.1 & 26.9 & 23.4 (C^{13}, C^{14}, C^{15}, C^{16}, C^{21}, C^{22}, C^{23}, C^{24}), 21.0 & 20.9 & 20.8 & 20.6 ppm (CH_3CO); HRMS (ESI): $[M-2PF_6]^{2+}$; calcd for $[C_{74}H_{108}N_6O_{18}]^{2+}$: 684.3860, found: 684.3841.

Acknowledgements

We are grateful to the French government and to the Ligue Nationale Contre le Cancer (LNCC) for PhD financial support.

[1] a) E. R. Kay, D. A. Leigh, F. Zerbetto, *Angew. Chem.* **2007**, *119*, 72–196; *Angew. Chem. Int. Ed.* **2007**, *46*, 72–191; b) D. A. Leigh, J. K. Y. Wong, F. Dehez, F. Zerbetto, *Nature* **2003**, *424*, 174–179; J. Berná, D. A. Leigh, M. Lubomska, S. M. Mendoza, E. M. Perez, P. Rudolf, G. Teobaldi, F. Zerbetto, *Nat. Mater.* **2005**, *4*, 704–710; c) J. V. Hernandez, E. R. Kay, D. A. Leigh, *Science* **2004**, *306*, 1532–1537; d) V. Serreli, C. F. Lee, E. R. Kay, D. A. Leigh, *Nature* **2007**, *445*, 523–527; e) B. Brough, B. H. Northrop, J. J. Schmidt, H.-R. Tseng, K. N. Houk, J. F. Stoddart, C.-M. Ho, *Proc. Natl. Acad. Sci. USA* **2006**, *103*, 8583–8588; f) V. Balzani, M. Clemente-Leon, A. Credi, B. Ferrer, M. Venturi, A. H. Flood, J. F. Stoddart, *Proc. Natl. Acad. Sci. USA* **2006**, *103*, 1178–1183; g) K. Galatsis, A. Khitun, R. Ostroumov, K. L. Wang, W. R. Dichtel, E. Plummer, J. F. Stoddart, J. I. Zink, J. Y. Lee, Y.-H. Xie, K. W. Kim, *IEEE Trans. Nanotechnol.* **2009**, *8*, 66–75; h) Y. Chen, G.-Y. Jung, D. A. A. Ohlberg, X. Li, D. R. Stewart, J. O. Jeppesen, K. A. Nielsen, J. F. Stoddart, R. S. Williams, *Nanotechnology* **2003**, *14*, 462–468; i) H. Kim, W. A. Goddard III, S. S. Jang, W. R. Dichtel, J. R. Heath, J. F. Stoddart, *J. Phys. Chem. A* **2009**, *113*, 2136–2143; j) Y. Luo, C. P. Collier, J. O. Jeppesen, K. A. Nielsen, E. Delonno, G. Ho, J. Perkins, H. R. Tseng, T. Yamamoto, J. F. Stoddart, J. R. Heath, *ChemPhysChem* **2002**, *3*, 519–525; k) J. E. Green, J. W. Choi, A. Boukai, Y. Bunimovich, E. Johnston-Halperin, E. Delonno, Y. Luo, B. A. Sheriff, K. Xu, Y. S. Shin, H. R. Tseng, J. F. Stoddart, J. R. Heath, *Nature* **2007**, *445*, 414–417; l) W. R. Dichtel, J. R. Heath, J. F. Stoddart, *Philos. Trans. R. Soc. London Ser. A* **2007**, *365*, 1607–1625; m) R. Beckman, K. Beverly, A. Boukai, Y. Bunimovich, J. W. Choi, E. DeIonno, J. Green, E. Johnston-Halperin, Y. Luo, B. Sheriff, J. F. Stoddart, J. R. Heath, *Faraday Discuss.* **2006**, *131*, 9–22; n) J. W. Choi, A. H. Flood, D. W. Steuerman, S. Nygaard, A. B. Braunschweig, N. N. P. Moonen, B. W. Laursen, Y. Luo, E. Delonno, A. J. Peters, J. O. Jeppesen, K. Xe, J. F. Stoddart, J. R. Heath, *Chem. Eur. J.* **2006**, *12*, 261–279; o) A. H. Flood, J. F. Stoddart, D. W. Steuerman, J. R. Heath, *Science* **2004**, *306*, 2055—2056.

[2] A. G. Kolchinski, D. H. Busch, N. W. Alcock, *J. Chem. Soc. Chem. Commun.* **1995**, 1289–1291.

[3] P. R. Ashton, P. J. Campbell, P. T. Glink, D. Philp, N. Spencer, J. F. Stoddart, E. J. T. Chrystal, S. Menzer, D. J. Williams, P. A. Tasker, *Angew. Chem.* **1995**, *107*, 1997–2001; *Angew. Chem. Int. Ed. Engl.* **1995**, *34*, 1865–1869.

[4] a) S. J. Loeb, J. Tiburcio, S. J. Vella, *Org. Lett.* **2005**, *7*, 4923–4926; b) D. A. Leigh, A. R. Thomson, *Org. Lett.* **2006**, *8*, 5377–5379.

[5] A. B. Braunschweig, C. M. Ronconi, J. Y. Han, F. Arico, S. J. Cantrill, J. F. Stoddart, S. I. Khan, A. J. P. White, D. J. Williams, *Eur. J. Org. Chem.* **2006**, 1857–1886.

[6] a) S. J. Loeb, J. Tiburcio, S. J. Vella, *Org. Biomol. Chem.* **2006**, *4*, 667–680; b) S. J. Loeb, *Chem. Soc. Rev.* **2007**, *36*, 226–235.

[7] F. Coutrot, E. Busseron, J.-L. Montero, *Org. Lett.* **2008**, *10*, 753–756.

[8] a) F. Coutrot, E. Busseron, *Chem. Eur. J.* **2008**, *14*, 4784–4787; b) F. Coutrot, C. Romuald, E. Busseron, *Org. Lett.* **2008**, *10*, 3741–3744; c) F. Coutrot, E. Busseron, *Chem. Eur. J.* **2009**, *15*, 5186–5190.

[9] For the first molecular brake which was not based on a multicomponent interlocked structure, see: T. R. Kelly, M. C. Bowyer, K. V. Bhaskar, D. Bebbington, A. Garcia, F. Lang, M. H. Kim, M. P. Jette, *J. Am. Chem. Soc.* **1994**, *116*, 3657–3658.

[10] a) R. Huisgen, *Pure Appl. Chem.* **1989**, *61*, 613–628; b) R. Huisgen, *Angew. Chem.* **1963**, *75*, 604–637; *Angew. Chem. Int. Ed. Engl.* **1963**, *2*, 565–598; c) R. Huisgen, G. Szeimies, L. Möbius, *Chem. Ber.* **1967**, *100*, 2494–2507; d) R. Huisgen, *Angew. Chem.* **1963**, *75*, 742–754; *Angew. Chem. Int. Ed. Engl.* **1963**, *2*, 633–645. For recent syntheses of rotaxanes by using a copper(I)-catalyzed azide–alkyne 1,3-cycloaddition strategy, see: e) V. Aucagne, K. D. Hänni, D. A. Leigh, P. J. Lusby, D. B. Walker, *J. Am. Chem. Soc.* **2006**, *128*, 2186–2187; f) P. Mobian, J.-P. Collin, J.-P. Sauvage, *Tetrahedron Lett.* **2006**, *47*, 4907–4909; g) A. B. Braunschweig, W. R. Dichtel, O. S. Miljanic, M. A. Olson, J. M. Spruell, S. I. Khan, J. R. Heath, J. F. Stoddart, *Chem. Asian J.* **2007**, *2*, 634–647; h) V. Aucagne, J. Berna, J. D. Crowley, S. M. Goldup, K. D. Hänni, D. A. Leigh, P. J. Lusby, V. E. Ronaldson, A. M. Z. Slawin, A. Viterisi, D. B. Walker, *J. Am. Chem. Soc.* **2007**, *129*, 11950–11963; i) I. Aprahamian, T. Yasuda, T. Ikeda, S. Saha, W. R. Dichtel, K. Isoda, T. Kato, J. F. Stoddart, *Angew. Chem.* **2007**, *119*, 4759–4763; *Angew. Chem. Int. Ed.* **2007**, *46*, 4675–4679; j) I. Aprahamian, O. Miljanic, W. R. Dichtel, K. Isoda, T. Yasuda, T. Kato, J. F. Stoddart, *Bull. Chem. Soc. Jpn.* **2007**, *80*, 1856–1869; k) I. Aprahamian, W. R. Dichtel, T. Ikeda, J. R. Heath, J. F. Stoddart, *Org. Lett.* **2007**, *9*, 1287–1290; l) O. S. Miljanic, W. R. Dichtel, I. Aprahamian, R. D. Rohde, H. D. Agnew, J. R. Heath, J. F. Stoddart, *QSAR Comb. Sci.* **2007**, *26*, 1165–1174; m) J. M.

 © 2010 Wiley-VCH Verlag GmbH & Co. KGaA, Weinheim

Spruell, W. R. Dichtel, J. R. Heath, J. F. Stoddart, *Chem. Eur. J.* **2008**, *14*, 4168–4177; n) W. Zhang, W. R. Dichtel, A. Z. Stieg, D. Benitez, J. K. Gimzewski, J. R. Heath, J. F. Stoddart, *Proc. Natl. Acad. Sci. USA* **2008**, *105*, 6514–6519.

[11] a) H. C. Kolb, M. G. Finn, K. B. Sharpless, *Angew. Chem.* **2001**, *113*, 2056–2075; *Angew. Chem. Int. Ed.* **2001**, *40*, 2004–2021; b) J. F. Lutz, *Angew. Chem.* **2008**, *120*, 2212–2214; *Angew. Chem. Int. Ed.* **2008**, *47*, 2182–2184.

[12] a) C. L. Perrin, *Tetrahedron* **1995**, *51*, 11901–11935; b) R. U. Lemieux, A. R. Morgan, *Can. J. Chem.* **1965**, *43*, 2205–2213; c) R. U. Lemieux, *Pure Appl. Chem.* **1971**, *25–28*, 527–547.

[13] The *trans*/*cis* ratio of the two diastereoisomers of **5b** was determined by a NOESY experiment (see Supporting Information).

[14] a) I. Yoon, D. Benitez, Y.-L. Zhao, O. S. Miljanic, S.-Y. Kim, E. Tkatchouk, K. C.-F. Leung, S. I. Khan, W. A. Goddard III, J. F. Stoddart, *Chem. Eur. J.* **2009**, *15*, 1115–1122; b) A. Credi, *J. Phys. Condens. Matter* **2006**, *18*, S1779–S1795; c) P. L. Anelli, N. Spencer, J. F. Stoddart, *J. Am. Chem. Soc.* **1991**, *113*, 5131–5133; d) P.-L. Anelli, M. Asakawa, P. R. Ashton, R. A. Bissell, G. Clavier, R. Górski, A. E. Kaifer, S. J. Langford, G. Mattersteig, S. Menzer, D. Philp, A. M. Z. Slawin, N. Spencer, J. F. Stoddart, M. S. Tolley, D. J. Williams, *Chem. Eur. J.* **1997**, *3*, 1113–1135; e) V. Balzani, A. Credi, B. Ferrer, S. Silvi, M. Venturi, *Top. Curr. Chem.* **2005**, *262*, 1–27.

[15] Preparation of uncomplexed dumbbell-shaped threads **5au**/**6au** and **5bu**/**6bu** is described in the Supporting Information.

[16] L. Fielding, *Tetrahedron* **2000**, *56*, 6151–6170.

[17] The calculated ratio $\mathbf{6a_1}/\mathbf{6a_2}$ corresponds to an average ratio based on H^8 and H^{18} (see Table 1).

[18] A. Pastor, E. Martinez-Viviente, *Coord. Chem. Rev.* **2008**, *252*, 2314–2345.

[19] The mean ratio $\mathbf{6a_1}/\mathbf{6a_2}$ (based on both H^{18} and H^8) was used for the determination of *K* for all the considered temperatures, with the exception of 233 K, for which the best fitted *K* value arose from H^{18}.

[20] M. Pons, O. Millet, *Prog. Nucl. Magn. Reson. Spectrosc.* **2001**, *38*, 267–324.

[21] S. Arrhenius, *Z. Phys. Chem. Stoechiom. Verwandtschaftsl.* **1889**, *4*, 226.

[22] H. Eyring, *Chem. Rev.* **1935**, *17*, 65.

[23] Very similar $\Delta G^{\neq}$ were reported for shuttling in peptide-based molecular machines containing two degenerate glycylglycine molecular stations, see: A. S. Lane, D. A. Leigh, A. Murphy, *J. Am. Chem. Soc.* **1997**, *119*, 11092–11093.

[24] *Dynamic NMR Spectroscopy* (Ed.: J. Sandstrom), Academic Press, New York, **1982**.

[25] The free enthalpy of activation was calculated by using the Eyring equation: $\Delta G_T^{\neq} = -RT\ln(kh/k_bT)$.

[26] *La spectroscopie de RMN* (Ed.: H. Günther), Masson, Paris, **1994**.

Received: March 27, 2010
Published online: July 6, 2010

 © 2010 Wiley-VCH Verlag GmbH & Co. KGaA, Weinheim